

1 **Spatio-temporal diversity of dietary preferences and stress sensibilities of early and middle**
2 **Miocene Rhinocerotidae from Eurasia: impact of climate changes**

3

4

5 Authors: M. Hullo¹, G. Merceron², P.-O. Antoine³

6

7 1- Bayerische Staatssammlung für Paläontologie und Geologie, Richard-Wagner Straße 10,

8 80333 Munich, Germany

9 2- PALEVOPRIM UMR 7262, CNRS, Université de Poitiers, 86073 Poitiers, France


10 3- Institut des Sciences de l'Évolution, UMR5554, Univ Montpellier, CNRS, IRD, Place Eugène

11 Bataillon, CC064, 34095 Montpellier, France

12

13 **Abstract**

14

15 Major climatic and ecological changes are documented in terrestrial ecosystems during the Miocene
16 epoch. The Rhinocerotidae are a very interesting clade to investigate the impact of these changes on
17 ecology, as they are abundant and diverse in the fossil record throughout the Miocene. Here, we
18 explored the spatio-temporal evolution of rhinocerotids' paleoecology during the early and middle
19 Miocene in Europe and Pakistan. We studied the dental texture microwear (proxy for diet) and enamel
20 hypoplasia (stress indicator) of 19 species belonging to four sub-tribes and an unnamed clade of
21 Rhinocerotidae, and coming from nine Eurasian localities ranging from MN2 to MN7/8. Our results
22 suggest a clear niche partitioning based on diet at Kumbi 4 (MN2, Pakistan), Sansan (MN6, France),
23 and Villefranche d'Astarac (MN7/8, France), while ~~dietary overlap~~ and subtle variations are discussed
24 for Béon 1 (MN4, France) and Gračanica (MN5/6, Bosnia-Herzegovina). All rhinocerotids studied were
25 ~~browsers or mixed-feeders, and none had a grazing nor frugivore diet. Regarding hypoplasia, the~~
26 ~~prevalence was moderate (~ 10%) to high (> 20 %) at all localities but Kumbi 4 (~ 6 %), and~~
27 documented quite well the local conditions. Sansan and Devínska Nová Ves (MN6, Slovakia), both
28 dated to the MN6 (i.e., by the middle Miocene Climatic Transition, ca. 13.9 Mya), had moderate 
29 hypoplasia prevalence. Besides locality, species and tooth locus were also important factors of
30 variation for the prevalence of hypoplasia. The very large hippo-like *Brachypotherium brachypus* was

31 one of the most affected species at all concerned localities (but Sansan), while early-diverging
32 elasmotheriines were very little affected.


33

34 **Keywords:** paleoecology, Miocene Climatic Optimum (MCO), microwear (DMTA), enamel hypoplasia



35

36 Introduction

37

38 The Miocene is a key period in Earth and rhinocerotid evolutionary histories. Climatic conditions in
39 Eurasia during the Miocene epoch are globally trop  and the typical habitat is forested (Cerling et
40 al., 1997; Zachos et al., 2001; Bruch et al., 2007; Westerhold et al., 2020). It is the last warm episode
41 of the Cenozoic era, although marked by great climatic changes prefiguring the setup of modern cold
42 conditions (Westerhold et al., 2020). During early Miocene times, temperatures increased until
43 reaching the Miocene Climatic Optimum (MCO) between ~17 to 14 Mya (corresponding to the late
44 Burdigalian + Langhian standard ages; Westerhold et al., 2020). This optimum is followed by an
45 abrupt cooling (the middle Miocene climatic transition [mMCT]; Westerhold et al., 2020) associated
46 with faunal turnovers in Eurasia (Böhme, 2003; Maridet et al., 2007). The middle Miocene is marked
47 by a relative aridity, associated with a global cooling (Bruch et al., 2007; Böhme et al., 2008).

48

49 Concerning rhinocerotids, Miocene times witness peaks in their alpha diversity about 22–18 Mya and
50 11–10 Mya (Antoine et al., 2010; Antoine and Becker, 2013; Antoine, in press). During the early and
51 middle Miocene in Eurasia, four sub-tribes of Rhinocerotidae are encountered – Rhinocerotina,
52 Teleoceratina and Aceratheriina (Rhinocerotinae), and Elasmotheriina (Elasmotheriinae) – and
53 species of which are often found associated in fossil-yielding localities (Antoine et al., 1997, 2010;
54 Heissig, 2012; Becker and Tissier, 2020; Antoine, 2002, in press). This abundance and the potential
55 cohabitation of such large herbivores question habitat capacity and competition for food resources.
56 However, the ecology of the rhinocerotids has rarely  been explored or only been assumed based on
57 morphological adaptations (Prothero et al., 1989; Prothero, 2005; Giaourtsakis et al., 2006). If the
58 Rhinocerotina appear to be ecologically varied, the literature suggests a similar ecology for most
59 elasmotheriines on one hand, as open environment dwellers adapted to tough vegetation (Iñigo and
60 Cerdeño, 1997; Antoine and Welcomme, 2000), and for the teleoceratines on another hand, as hip 

61 like rhinoceroses inhabiting lake side or swamps and probably browsing on low vegetation or even
62 grazing (Prothero et al., 1989; Cerdeño, 1998).

63

64 In this article, we focused on the rhinocerotids from nine localities, covering wide temporal and
65 geographical ranges (from MN2 to MN7/8 and from southwestern France to Pakistan). We assessed
66 dietary preferences using dental microwear texture analysis, and stress sensibility via the study of
67 enamel hypoplasia.

68

69 **Material and methods**

70

71 We studied the rhinocerotid dental remains from nine early and middle Miocene localities from France
72 (Béon 1, Béon 2, Sansan, Simorre, and Villefranche d'Astarac), Germany (Steinheim am Albuch),
73 Bosnia-Herzegovina (Gračanica), Slovakia (Devínska Nová Ves Spalte), and Pakistan (Kumbi 4,
74 Balochistan), ranging from MN2 to MN7/8. The rhinocerotid assemblages are detailed in Table 1. The
75 specimens are curated at the Naturhistorisches Museum Wien (NHMW), the Muséum de Toulouse
76 (MHNT), and the Naturhistorisches Museum Basel (NHMB). For all details on the specimens included
77 in this study see Supplementary S1. The localization of the studied localities is given in Figure 1.
78 Further details on the localities are given in Supplementary S2.

79

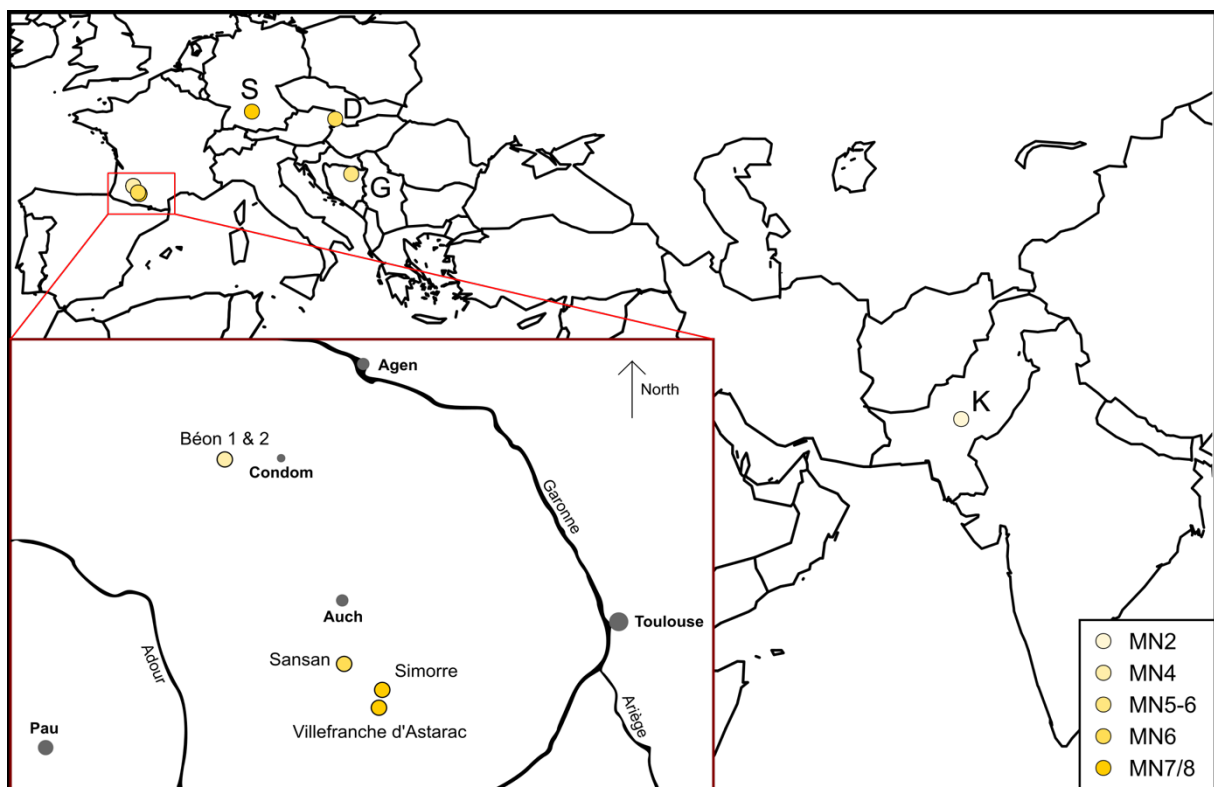
80 Dental Microwear Texture Analyses (DMTA)

81 Dental Microwear Texture Analysis (DMTA) is a powerful approach to characterize dietary preferences
82 at a short time scale (days to weeks prior the death of the individual; Hoffman et al., 2015; Winkler et
83 al., 2020), widely used in paleontological and archeological studies (Grine, 1986; Rivals et al., 2012;
84 Jones and DeSantis, 2017; Berlioz et al., 2018). We studied dental microwear texture on one well-
85 preserved molar (germs and over-worn teeth excluded) per individual, preferentially the second molar
86 (first or third otherwise), either upper or lower, left or right.

87

88 After cleaning the tooth with acetone or ethanol, two silicone (Regular Body President, ref. 6015 - ISO
89 4823, medium consistency, polyvinylsiloxane addition type; Coltene Whaledent) molds were made on
90 a single enamel band, which shows two different facets acting as grinding and shearing (if present).

91 This shearing facet has a steep slope while the former is more horizontal and show several HSB band
92 on the very enamel surface. To combine both type of facets with different functions indeed improves
93 dietary reconstruction (Louail et al., 2021; Merceron et al., 2021). The enamel band on which we
94 identified those two facets is localized labially near the protocone on upper molars and distally to the
95 protoconid or hypoconid (if the protoconid is unavailable) on lower teeth (see supplementary S2).
96
97



98

99 **Figure 1: Geographical position of the studied Eurasian Miocene localities.**

100 Localization of all localities in Eurasia. Red square is a zoom on the southwestern French localities,
101 modified from Antoine and Duranthon (1997).

102 Color code by MN zones as detailed in A. Abbreviations from West to East: S- Steinheim am Albuch
103 (MN7/8; Germany), D- Devínska Nová Ves Spalte (MN6; Slovakia), G- Gračanica (MN5-6; Bosnia-
104 Herzegovina), K- Kumbi 4 (MN2; Pakistan).

105 **Table 1: List of rhinocerotid species found at each locality studied**

	Kumbi 4	Béon 2	Béon 1	Gračanica	Sansan	Devínska Nová Ves Spalte	Steinheim am Albuch	Simorre	Villefranche d'Astarac
Rhinocerotinae									
<i>Mesaceratherium welcommi</i>	x								
<i>Pleuroceros blanfordi</i>	x								
<i>Protaceratherium</i> sp.	x								
<i>Protaceratherium minutum</i>		x							
<i>Plesiaceratherium naricum</i>	x								
<i>Plesiaceratherium mirallesi</i>		x	x						
<i>Plesiaceratherium balkanicum</i>				x		x			
<i>Plesiaceratherium</i> sp.			x						
Aceratheriina									
<i>Hoploaceratherium tetradactylum</i>					x				
<i>Alicornops simorreense</i>					x		x	x	x
Rhinocerotina									
<i>Gaindatherium</i> cf. <i>browni</i>	x								
<i>Lartetotherium sansaniense</i>				x	x		x		
<i>Dicerorhinus steinheimensis</i>						x	x		
Teleoceratina									
<i>Brachypotherium brachypus</i>			x	x	x		x	x	x
<i>Brachypotherium gajense</i>	x								
<i>Diaceratherium fatehjangense</i>	x								
<i>Prosantorhinus douvillei</i>		aff.	x						
<i>Prosantorhinus shahbazi</i>	x								
Elasmotheriinae									
Elasmotheriina									
<i>Bugtirhinus praecursor</i>	x								
<i>Hispanotherium beonense</i>			x						
<i>Hispanotherium</i> cf. <i>matritense</i>				x					
Total	9	3	5	4	4	2	4	2	2

106

107

108 In this article we followed a protocol adapted from Scott et al. (2005, 2006) with sensitive-scale fractal

109 analyses. Molds were scanned with a Leica DCM8 confocal profilometer ("TRIDENT" profilometer

110 housed at the PALEVOPRIM, CNRS, University of Poitiers) using white light confocal technology with

111 a 100× objective (Leica Microsystems; Numerical aperture: 0.90; working distance: 0.9 mm). The

112 obtained scans (.plu files) were pre-treated with LeicaMap v.8.2. (Leica Microsystems) as follows: the
113 surface was inverted (as scans were made on negative replicas), missing points (i.e., non-measured,
114 less than 1%) were replaced by the mean of the neighboring points and aberrant peaks were removed
115 (see details in the supplementary Information in Merceron et al., 2016b). The surface was then
116 levelled, and we applied a polynomial of degree 5 removal of form to temper for Hunter-Schreger
117 bands reliefs in the DMTA parameters. Eventually, we selected a 200×200-µm area (1551 × 1551
118 pixels) within the surface, which we saved as a digital elevation model (.sur) and used to extract
119 DMTA parameters through Scale-Sensitive Fractal Analysis with SFrax (Surfract, www.surfract.com)
120 and LeicaMap.

121
122 Here we focused on five classical DMTA parameters: anisotropy (exact proportion of length-scale
123 anisotropy of relief; epLsar), complexity (area-scale fractal complexity; Asfc), heterogeneity of
124 complexity (heterogeneity of area-scale fractal complexity here at 3×3 and 9×9; HASfc9 and HASfc81),
125 and fine textural fill volume (here at 0.2 µm; FTfv). The description of these parameters is available in
126 Scott et al. (2006).

127
128 To facilitate DMTA interpretation for fossil specimen, we used specimens of the five extant rhinocerotid
129 species. This extant dataset was modified from that of Hullot et al. (2019), as precised below, and
130 consists of 17 specimens of *Ceratotherium simum* (white rhinoceros), four of *Dicerorhinus sumatrensis*
131 (Sumatran rhinoceros), 21 of *Diceros bicornis* (black rhinoceros), 15 of *Rhinoceros sondaicus* (Javan
132 rhinoceros; one new specimen), and five of *Rhinoceros unicornis* (Indian rhinoceros; one new
133 specimen).

134

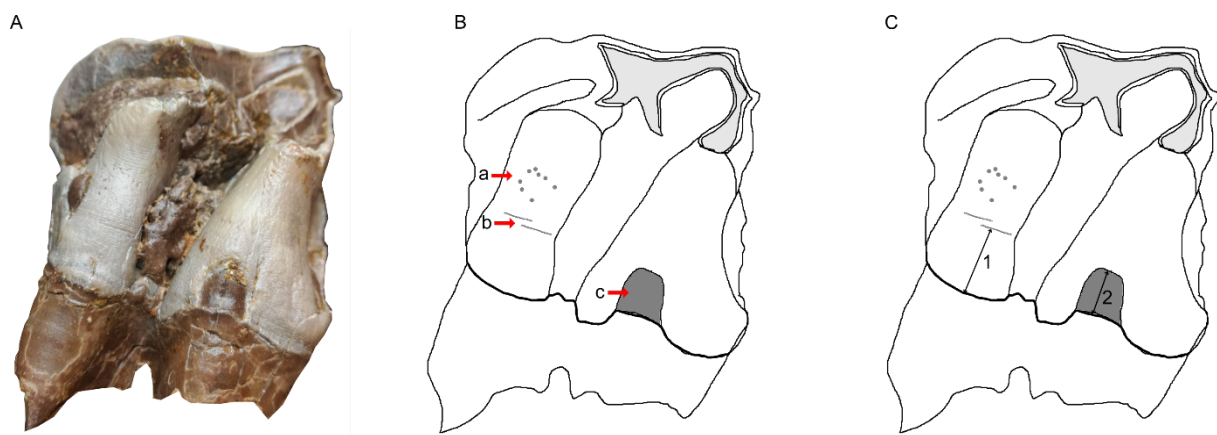
135 Enamel hypoplasia

136 Hypoplasia is a common defect of the enamel resulting from a stress or a combination of stresses
137 occurring during tooth development (Goodman and Rose, 1990). It is a permanent, sensitive, but non-
138 specific indicator of stresses either environmental (e.g., drought or nutritional stress; Skinner and
139 Pruetz, 2012; Upex and Dobney, 2012), physiological (e.g., disease or parasitism; Suckling et al.,
140 1986; Rothschild et al., 2001; Niven et al., 2004), and/or psychological (e.g., depression in primates;
141 Guatelli-Steinberg, 2001).

142 Enamel hypoplasia was studied with the naked eye and categorization of the defects followed the
143 *Fédération Dentaire Internationale* (1982) as linear enamel hypoplasia (LEH), pitted hypoplasia, or
144 aplasia. We studied all cheek teeth, both deciduous and permanent, but excluded 62 teeth to avoid
145 false negative and uncalibrated defects, as enamel was obscured (e.g., tooth unerupted in bone,
146 sediment occluding), broken or worn out, or as identification was impossible. This left 1401 teeth
147 studied for the hypoplasia analysis – 294 milk molars and 1107 permanent premolars and molars –
148 from the nine localities. In parallel, qualitative data (tooth locus affected, position of the defect on the
149 crown, and severity) and caliper measurements (distance of the defect from enamel-dentine junction,
150 width if applicable) were taken (details in Supplementary S3). Type of defects recorded, and caliper
151 measurements are illustrated in Figure 2.

152

153



154

155

156 **Figure 2: The three different types of hypoplasia considered in this study and the associated**
157 **measurements**

158 A- Lingual view of right M2 of the specimen MHNT.PAL.2004.0.58 (*Hispanotherium beonense*)

159 displaying three types of hypoplasia

160 B- Interpretative drawing of the photo in A illustrating the hypoplastic defects: a- pitted hypoplasia, b-
161 linear enamel hypoplasia, and c- aplasia

162 C- Interpretative drawing of the photo in A illustrating the measurements: 1- distance between the
163 base of the defect and the enamel-dentin junction, 2- width of the defect (when applicable).

164 Figure from Hullot et al. (2021).

165

166 Statistics and GLMMs

167 Statistics were conducted in R (R Core Team, 2018: <https://www.R-project.org/>), equipped with the
168 following packages: reshape2 (Wickham, 2007), dplyr (Wickham et al., 2019), lme4 (Bates et al.,
169 2015), car (Fox et al., 2012), MASS (Venables and Ripley, 2002). According to the recent statement of
170 the American Statistical Association (ASA) on p-values (Wasserstein and Lazar, 2016; Wasserstein et
171 al., 2019), we avoided the use of the term “statistically significant” in this manuscript and the classical
172 thresholds as much as possible. Figures were done using R package ggplot2 (Wickham, 2011) as well
173 as Inkscape v.0.91.

174

175 General Linear Mixed Models (GLMM) on our data were constructed based on a R code modified from
176 Arman et al. (2019) and adapted to each tested response variable. An example of this code applied to
177 hypoplasia variable Hypo is given in Supplementary 4. DMTA response variables were the five DMTA
178 parameters (epLsar, Asfc, FTfv, HAsfc9, and HAsfc81) and we selected Gaussian family for the
179 GLMMs. Factors in the models were: specimen (number of the specimen; random factor), locality,
180 province, age (MN zones), genus, tooth (e.g., second molar, fourth milk molar), position (upper or
181 lower), side (left or right), cusp (protocone, protoconid, hypoconid), and facet (grinding or shearing).
182 For hypoplasia, response variables were Hypo (1 or 0 for presence or absence of hypoplasia,
183 respectively) for which we used Binomial family, Defect (e.g., LEH, Pits, Aplasia; converted to
184 numbers), Localization (position of the defect on the crown; mostly labial or lingual), Multiple (number
185 of defects), and Severity (0 to 4), modeled using Poisson family. The factors were: specimen (number
186 of the specimen; random factor), locality, province, age (MN zones), genus, tooth (e.g., first molar,
187 fourth premolar), position (upper or lower), side (left or right), and wear (low, average, high).
188 Additionally, for response variables Severity, Multiple, and Localization, defect was converted and
189 used as a factor.

190

191 The models were built with a bottom-up approach, starting with the only random factor of our dataset
192 alone (specimen) and adding factors incrementally for every set (e.g., 1|Specimen + Genus,
193 1|Specimen + Locality). New set was built as long as Akaike's Information Criterion score (AIC) kept
194 decreasing. Few interactions (e.g., Genus x Facet for microwear, Genus x Tooth for hypoplasia) were
195 considered in the models, as most factors were considered independent and to avoid unnecessarily

196 complex and rarely selected models (Arman et al., 2019). We selected the best candidate model as
197 the one with the lowest AIC and checked for over-dispersion (estimated through the ratio of deviance
198 and degrees of freedom). If needed, we corrected it through quasi-Poisson or quasi-Binomial laws
199 from the MASS package (Venables and Ripley, 2002) or by adjusting the coefficients table (multiply
200 type error by square root of the dispersion factor and recalculate Z and p values accordingly). In total,
201 340 models were compared across the 10 response variables (see electronic supplementary material,
202 S5, S6, and S7).

203

204 **Results**

205

206 Microwear

207 MANOVA (Species x Facet x Age x Locality) on all five main DMTA parameters (epLsar, Asfc, FTfv,
208 HASfc9, HASfc81) revealed low p-values for Species (df = 14; p-value = 8.6×10^{-4}), Facet (df = 1; p-
209 value = 6.5×10^{-4}), and Locality (df = 4; p-value = 0.014). The ANOVAs for each parameter,
210 highlighted at least a marked influence of Species (all parameters; p-values between 7.3×10^{-4} and
211 0.027), Facet (Asfc, p-value = 0.028; FTfv, p-value = 6.22×10^{-6}), Age (Asfc, p-value = 7.57×10^{-3}), or
212 Locality (epLsar, p-value = 0.01; Asfc, p-value = 1.7×10^{-4}). To precise the differences for Species and
213 Locality (factors with more than two states) we ran post hocs, results of which are detailed in Table 2
214 and Table 3. The more conservative post hoc (Tukey's honestly significant difference; HSD) revealed
215 very few noticeable differences in the microwear textures of the studied rhinocerotid specimens by
216 Species or Locality (low p-values relatively to other pairs; Table 2). The DMT of *Hoploaceratherium*
217 *tetradactylum* appears quite distinct from that of *Plesiaceratherium* spp. (epLsar, Asfc, HASfc9 and
218 HASfc81). Concerning Locality, Gračanica specimens stood out with very low values of complexity
219 compared to Sansan (p-value = 0.047), Simorre (p-value = 0.028), and Villefranche d'Astarac (p-value
220 = 0.032).

221


222 The least conservative post hoc (Fischer's least significant difference; LSD) highlighted more
223 differences in the DMTA patterns of the specimens regarding Species and Locality (Table 3).

224 *Alicornops simorreense* and *P. mirallesi* cluster together with higher anisotropy than *P. douvillei*, *B.*

225 *brachypus*, *B. gajense*, *M. welcommi*, *D. steinheimensis*, *H. tetradactylum*, and *L. sansaniense* (Table

226 3; p-value < 0.05). Concerning complexity, *B. gajense* and *H. tetradactylum* stood out for having
 227 higher complexities compared to all other species besides *M. welcommi* and *G. cf. browni*. Moreover,
 228 *G. cf. browni* was different from *B. brachypus*, both *Plesiaceratherium* species, and both
 229 *Hispanotherium* species regarding complexity and HAsfc81 (Table 3). For both DMTA parameters in
 230 which Locality had a noticeable effect (epLsar and Asfc), we found a cluster between Béon 1 and
 231 Gračanica opposed to one containing at least Simorre and Sansan (for Asfc: also Kumbi 4 and
 232 Villefranche d'Astarac; Table 3).

233 **Table 2: Pairs (Species or Locality) with noticeable p-values after Tukey's honestly significant**
 234 **difference (HSD) by DMTA parameters.**

235 FT  not precised as it yielded p-values above 0.1 only

236

DMTA parameter	Pair (Species or Locality) with differences		p-value
Anisotropy	<i>Plesiaceratherium mirallesi</i>	<i>Brachypotherium brachypus</i>	0.066
		<i>Lartetotherium sansaniense</i>	0.054
		<i>Hoploaceratherium tetradactylum</i>	0.09
Complexity	Gračanica	<i>Hoploaceratherium tetradactylum</i>	<i>Hispanotherium beonense</i> 0.008
			<i>Prosantorhinus douvillei</i> 0.01
			<i>Plesiaceratherium mirallesi</i> 6.3 x 10 ⁻⁴
			<i>Plesiaceratherium balkanicum</i> 0.051
			Sansan 0.047
			Simorre 0.028
	Villefranche d'Astarac 0.032		
HAsfc9	<i>Hoploaceratherium tetradactylum</i>	<i>Plesiaceratherium balkanicum</i>	0.059
		<i>Plesiaceratherium mirallesi</i>	0.024
HAsfc81	<i>Hoploaceratherium tetradactylum</i>	<i>Plesiaceratherium balkanicum</i>	0.096
		<i>Plesiaceratherium mirallesi</i>	0.072

237

238 **Table 3: Fischer's least significant difference (LSD) post hoc results by DMTA parameters**

239 Groups (a, ab, abc, b, bc, and c) are indicated with a p-value threshold of 0.05, for the sake of clarity.

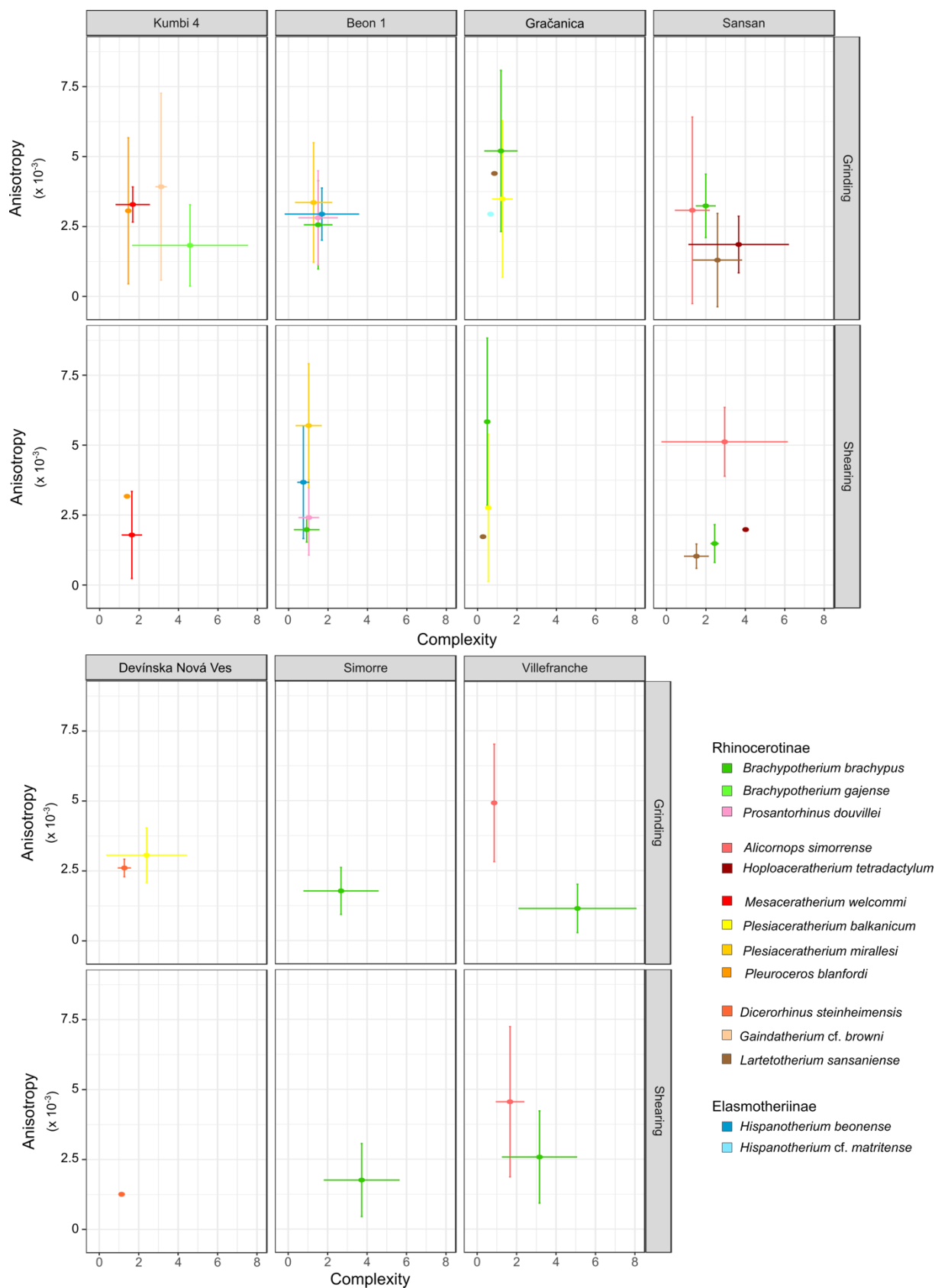
		a	ab	abc	b	bc	c
epLsar	Species	<i>A. simorrense</i> <i>P. mirallesi</i>	<i>G. cf. browni</i> <i>H. beonense</i> <i>H. cf. matritense</i> <i>P. balkanicum</i> <i>P. blanfordi</i>	-	<i>P. douvillei</i> <i>B. brachypus</i> <i>B. gajense</i> <i>M. welcommi</i> <i>D. steinheimensis</i> <i>L. sansaniense</i> <i>H. tetradactylum</i>	-	-
	Locality	Gračanica Béon 1	Villefranche d'Astarac Devínska Nová Ves Kumbi 4	-	Sansan Simorre	-	-
Asfc	Species	<i>B. gajense</i> <i>H. tetradactylum</i>	<i>G. cf. browni</i>	<i>M. welcommi</i>	-	<i>B. brachypus</i> <i>P. blanfordi</i> <i>A. simorrense</i> <i>D. steinheimensis</i> <i>L. sansaniense</i>	<i>P. douvillei</i> <i>P. balkanicum</i> <i>P. mirallesi</i> <i>H. beonense</i> <i>H. cf. matritense</i>
	Locality	Simorre Sansan Kumbi 4 Villefranche d'Astarac	Devínska Nová Ves	-	-	Béon 1	Gračanica
FTfv	Species	<i>H. cf. matritense</i> <i>B. gajense</i>	<i>P. blanfordi</i> <i>M. welcommi</i> <i>G. cf. browni</i> <i>D. steinheimensis</i> <i>H. tetradactylum</i> <i>P. douvillei</i> <i>H. beonense</i>	-	<i>B. brachypus</i> <i>A. simorrense</i> <i>P. balkanicum</i> <i>P. mirallesi</i> <i>L. sansaniense</i>	-	-
	Species	<i>G. cf. browni</i> <i>L. sansaniense</i> <i>H. tetradactylum</i>	<i>P. blanfordi</i> <i>B. gajense</i> <i>B. brachypus</i> <i>P. douvillei</i> <i>M. welcommi</i> <i>A. simorrense</i> <i>D. steinheimensis</i> <i>H. beonense</i>	-	<i>P. balkanicum</i> <i>P. mirallesi</i> <i>H. cf. matritense</i>	-	-
HAAsfc9	Species	<i>G. cf. browni</i> <i>L. sansaniense</i> <i>H. tetradactylum</i>	<i>P. blanfordi</i> <i>P. douvillei</i> <i>M. welcommi</i> <i>A. simorrense</i> <i>D. steinheimensis</i> <i>H. beonense</i>	-	<i>P. balkanicum</i> <i>P. mirallesi</i> <i>H. cf. matritense</i>	-	-
HAAsfc81	Species	<i>G. cf. browni</i>	<i>B. gajense</i> <i>H. tetradactylum</i> <i>L. sansaniense</i>	<i>P. blanfordi</i> <i>P. douvillei</i> <i>M. welcommi</i> <i>A. simorrense</i> <i>D. steinheimensis</i>	-	<i>B. brachypus</i> <i>H. beonense</i>	<i>P. balkanicum</i> <i>P. mirallesi</i> <i>H. cf. matritense</i>

240

241 Besides at Béon 1, the microwear sampling was very restricted ($n < 5$), either due to low numbers of
242 exploitable teeth available, or to the lack of well-preserved microwear texture on molars. In order to
243 facilitate the understanding, the results are presented by locality (chronologically) and by species. At
244 **Kumbi 4**, four species were considered for DMTA: *Pleuroceros blanfordi*, *Mesaceratherium welcommi*,
245 *Gaindatherium cf. browni* (grinding only), and *Brachypotherium gajense* (grinding only). Figure 3
246 shows that Kumbi rhinocerotids display a great variety of microwear patterns. Only one specimen,
247 belonging to *G. cf. browni*, is above the high anisotropy threshold of 5×10^{-3} , while all specimens of *B.*
248 *gajense* and *G. cf. browni* but none of *P. blanfordi* display values above the high complexity cutpoint of
249 2. *Gaindatherium cf. browni* and *P. blanfordi* have large variations in anisotropy, from low values ($\sim 1 \times$
250 10^{-3}) to high (about 5×10^{-3}), but consistent values of complexity (around 3 and 1.4 respectively). Such
251 a pattern associated with moderate (*P. blanfordi*) to high (*G. cf. browni*) values of HAsfc (Figure 4)
252 point towards mixed-feeding diets, probably with the inclusion of harder objects for *G. cf. browni*. The
253 signature for *B. gajense* is suggestive of browsing with low mean anisotropy (1.82×10^{-3}), but high
254 means of complexity (4.58), FTfv (7.89×10^4), and HAsfc (HAsfc9 = 0.36; HAsfc81 = 1). Eventually, *M.*
255 *welcommi* presents low to moderate anisotropy values ($< 4 \times 10^{-3}$), a moderate complexity (~ 1.5) and
256 HAsfc, but high FTfv ($> 4 \times 10^4$) on both facets (Figure 4), which denotes browsing or mixed-feeding
257 habits.

258

259 At **Béon 1**, the DMT of the four rhinocerotids overlap contrary to that of Kumbi 4 rhinocerotids (Figure
260 3). The DMTA results are already detailed in Hullot et al. (2021). They suggest a mixed-feeding
261 behavior for *H. beonense* with moderate anisotropy values (mostly $< 4 \times 10^{-3}$), variable values of
262 complexity (low-medium), moderate-high FTfv (around 4×10^4), and moderate HAsfc on both facets
263 (Figure 4). *Plesiaceratherium mirallesi* is considered as a folivore due to low complexity (~ 1) and
264 HAsfc values but relatively high anisotropy (above 5×10^{-3}), indicating an abrasive but not diversified
265 diet. Concerning the teleoceratines, they display similar microwear textures (Figure 3; Figure 4),
266 though *B. brachypus* has lower values of anisotropy ($< 2 \times 10^{-3}$). This suggests that *B. brachypus* was
267 probably a browser or a mixed-feeder, while *Pr. douvillei* was a browser favoring leaves.

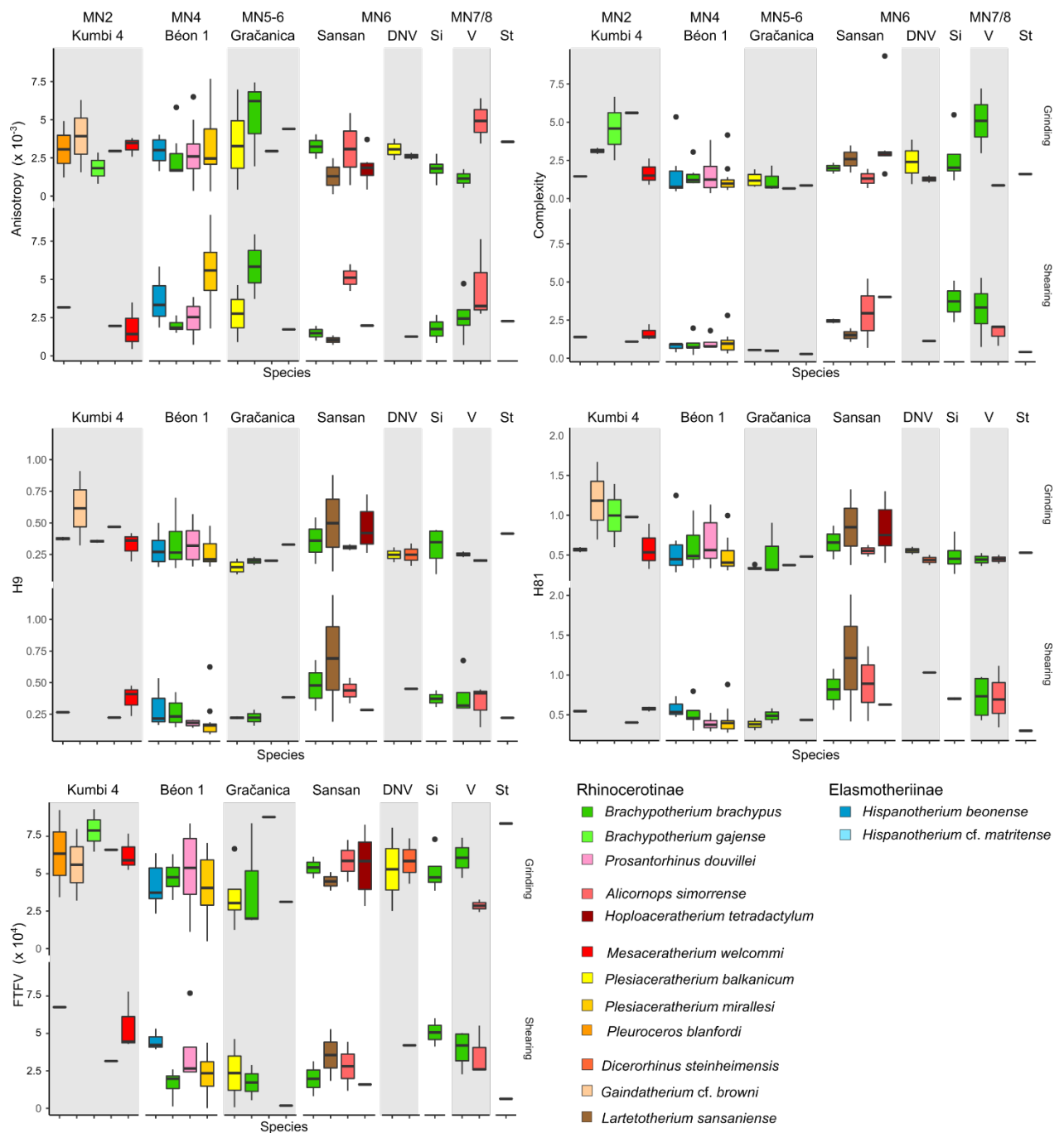


268

269 **Figure 3: Dental microwear results of early and middle Miocene rhinocerotids plotted as mean**

270 **and standard deviation of anisotropy against that of complexity by facet, locality and species**

271 Localities organized chronologically. Steinheim am Albuch not shown as only one specimen was
 272 studied. Color code by species as indicated in the figure.
 273



274
 275 **Figure 4: Dental microwear results of early and middle Miocene rhinocerotids plotted as**
 276 **boxplots of each DMTA parameter by facet and species.**

277 Time flows from left to right. DNV: Devínska Nová Ves, St: Steinheim am Albuch, Si: Simorre, V:
 278 Villefranche d'Astarac. Color code by species as indicated in the figure and consistent with Figure 3.

279 At **Gračanica**, we also observe a great overlapping in the DMT. The complexity is very low for all
280 rhinocerotids studied (mostly below 1) suggesting soft food items. Anisotropy varies greatly but
281 HAsfc81 is consistently low (< 0.5) for all species (Figure 4). This points towards soft browsing or
282 folivory for all rhinocerotids at Gračanica.

283

284 At **Sansan**, the DMTA signatures of the rhinocerotids are more diversified and less overlapping,
285 similarly to Kumbi 4 (Figure 3). *Lartetotherium sansaniense* and *H. tetradactylum* have low values of
286 anisotropy ($< 2.5 \times 10^{-3}$) and moderate (1-2; *L. sansaniense*) to high (> 2 ; *H. tetradactylum*) values of
287 complexity, recalling browsers. The high values of HAsfc (Figure 4) for both species are compatible
288 with a browsing diet. The other two species, *B. brachypus* and *A. simorreense*, are in the range of
289 mixed-feeders (Figure 3), and have compatible moderate to high values of HAsfc.

290

291 At **Devínska Nová Ves**, our restricted sample suggest browsing habits for both species *P. balkanicum*
292 and *D. steinheimensis*, with moderate values of both anisotropy ($\sim 2.5 \times 10^{-3}$) and complexity (mostly
293 between 1 and 1.5). FTfv is high on both facets ($> 4 \times 10^4$) and HAsfc moderate (Figure 3; Figure 4).

294

295 At **Simorre**, *B. brachypus* specimens display low values of anisotropy ($< 2.5 \times 10^{-3}$ except two
296 specimens), and high values of complexity (> 2) and FTfv ($> 4 \times 10^4$) on both facets. Values of HAsfc9
297 are high (> 0.3) on both facets, while that of HAsfc81 are moderate on the grinding facet (median =
298 0.45) and high on the shearing one (median = 0.7). These DMTA results suggest browsing
299 preferences with the inclusion of hard objects, probably fruits.

300

301 At **Villefranche d'Astarac**, *B. brachypus* and *A. simorreense* present well-distinguished DMT (Figure
302 3). *Brachypotherium brachypus* has low anisotropy values ($< 2.5 \times 10^{-3}$) and high complexity ones ($>$
303 2.5) corresponding to a browsing signal, while the opposite is true for *A. simorreense*. The moderate
304 values of HAsfc for *A. simorreense* suggest that folivory is more likely than mixed-feeding for these
305 specimens and the corresponding individuals.

306

307 Eventually the specimen of *A. simorreense* from **Steinheim am Albuch** has a moderate anisotropy
308 (Grinding: 3.56×10^{-3} ; Shearing: 2.27×10^{-3}), low (Shearing: 0.41) to moderate (Gringing: 1.6)

309 complexity, a high FTfv on the grinding facet (8.35×10^4) but low on the shearing one (0.63×10^4), and
310 low HASfc on the shearing facet but moderate-high on the grinding one (Figure 4). This pattern is
311 consistent with browsing or mixed-feeding habits.

312

313 **GLMM:** For all response variables (epLsar, Asfc, FTfv, HASfc9, and HASfc81), model support
314 increased (i.e., lower AIC) when intraspecific factors (e.g., Facet, Genus, Locality) were included. The
315 final models contained three to seven factors, including Specimen, the random factor, by default in all
316 models. Facet was in the final models of epLsar and FTfv, Locality and Age were found in the final
317 models of Asfc and both HASfc. Details and comparison of all models can be seen in electronic
318 supplementary material S5 and S6. Differences by Locality were also observed. Béon 1 had a lower
319 complexity than Kumbi 4, Sansan, Simorre, and Villefranche ($df = 119$, $\alpha = 0.05$, $|t\text{-values}| > 1.7$),
320 while Tukey's contrasts highlighted lower values of Asfc for Gračanica than for Kumbi ($p\text{-value} <$
321 0.004), Simorre ($p\text{-value} = 0.027$), and Villefranche ($p\text{-value} < 0.001$). Moreover, Béon 1 had lower
322 HASfc9 and HASfc81 values than Kumbi 4 and Sansan ($df = 119$, $\alpha = 0.05$, $|t\text{-values}| > 1.7$). Tukey's
323 contrasts also showed that Sansan had higher HASfc9 and HASfc81 than Gračanica ($p\text{-value} \leq 0.001$).
324 The sampling site (tooth locus, position, side) had sometimes a confounding effect. For instance, M2
325 had higher epLsar values than M3 ($df = 119$, $\alpha = 0.05$, $t\text{-value} = -1.95$).

326

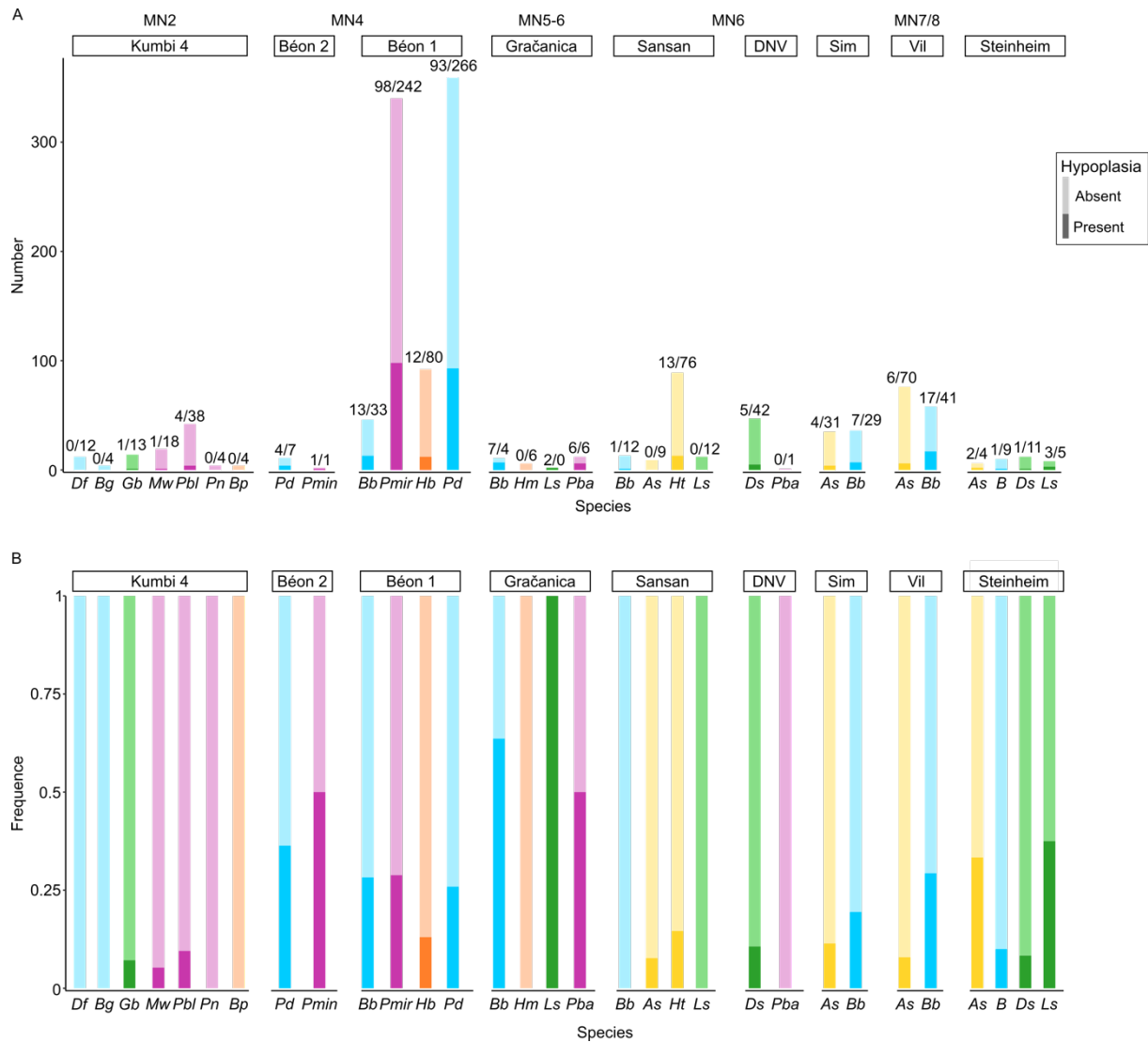
327 **GLMM - Comparison to extant dataset:** When compared to the extant dataset (see S8 for all
328 details), we noticed that all fossil species had lower anisotropy values than the extant grazer
329 *Ceratotherium simum* (white rhinoceros) and the folivore *Dicerorhinus sumatrensis* (Sumatran
330 rhinoceros), although the classic t-value threshold was not reached for a few species (*P. blanfordi*, *G.*
331 *cf. browsi*, *B. gajense* [only regarding *C. simum*], *P. mirallesi*, and *A. simorreense*; $\alpha = 0.95$, $|t\text{-values}| \leq$
332 1.7). On the contrary, *P. mirallesi* displayed higher values of anisotropy than the extant browsers
333 *Diceros bicornis* (black rhinoceros; $t\text{-value} = 1.93$) and *Rhinoceros sondaicus* (Javan rhinoceros; $t\text{-value} =$
334 2.66). Regarding complexity, *C. simum* and *D. sumatrensis* had lower values than *B. gajense*
335 and *H. tetradactylum*, while the extant browsers had higher values than *P. balkanicum*, *P. douvillei*, *P.*
336 *mirallesi*, and *H. beonense* ($\alpha = 0.95$, $|t\text{-values}| > 1.7$). All other DMTA parameters showed less
337 differences between the extant and fossil datasets: *C. simum* and *R. sondaicus* had higher FTfv,
338 HASfc9, and HASfc81 than *B. brachypus*, *P. balkanicum*, and *P. mirallesi* ($\alpha = 0.95$, $|t\text{-values}| > 1.7$).

339 Hypoplasia

340 The overall prevalence of hypoplasia on rhinocerotid teeth from the early and middle Miocene
341 localities studied is high, with 302 teeth affected out of 1401, corresponding to over 20 % (21.56 %).
342 There are, however, marked discrepancies between species, localities, and tooth loci (Figure 5). The
343 most affected genera were *Plesiaceratherium* (104/357; 29.13 %), *Prosantorhinus* (97/370; 26.22 %),
344 and *Brachypotherium* (46/178; 25.84 %), but this resulted mostly from the dominance of Béon 1
345 specimens in our sample. *Brachypotherium brachypus* was often one of the most affected species at
346 all sites where the species was found, except Sansan (1/13; 7.69 %), contrary to *A. simorreense* often
347 found associated with the latter species and relatively spared by hypoplasia (maximum 4/35 = 11.43 %
348 of teeth affected at Simorre; Figure 6).

349
350 The prevalence was above 10 % for all localities except Kumbi 4, for which the overall prevalence is
351 low (6/99; 6.06 %; Table 4). Hypoplasia defects are quite rare at Kumbi 4 for all species studied, and
352 even null for the teleoceratine species (*D. fatehjangense* and *B. gajense*), *Bugtirhinus praecursor*, and
353 *Plesiaceratherium naricum* (Figure 6). Only *Pleuroceros blanfordi* appears a little more affected (4/42;
354 9.52 %), totaling four of the six hypoplasias observed at the locality. Hypoplasia was also relatively
355 limited at Sansan (14/132; 10.61 %) and Devínska Nová Ves (5/48; 10.42 %), with only *B. brachypus*
356 and *H. tetradactylum* affected at Sansan, and *D. steinheimensis* from the latter (Table 4 ; Figure 6). On
357 the contrary, the rhinocerotids from Béon 1, Béon 2, and Gračanica are very affected, with more than
358 25 % of the teeth presenting at least one hypoplasia at Béon 1 (216/832; 25.96 %) and Béon 2 (5/18;
359 27.78 %), and nearly 50 % at Gračanica (15/31; 48.39 %; Table 4). At these sites, the prevalence of
360 hypoplasia is high for all species but the elasmotheriines (Figure 6). Indeed, the elasmotheriines of all
361 sites were relatively spared (*H. beonense* at Béon 1: 13.04 %) or even not affected by hypoplasia (*B.*
362 *praecursor* at Kumbi 4 and *H. cf. matritense* at Gračanica).

363

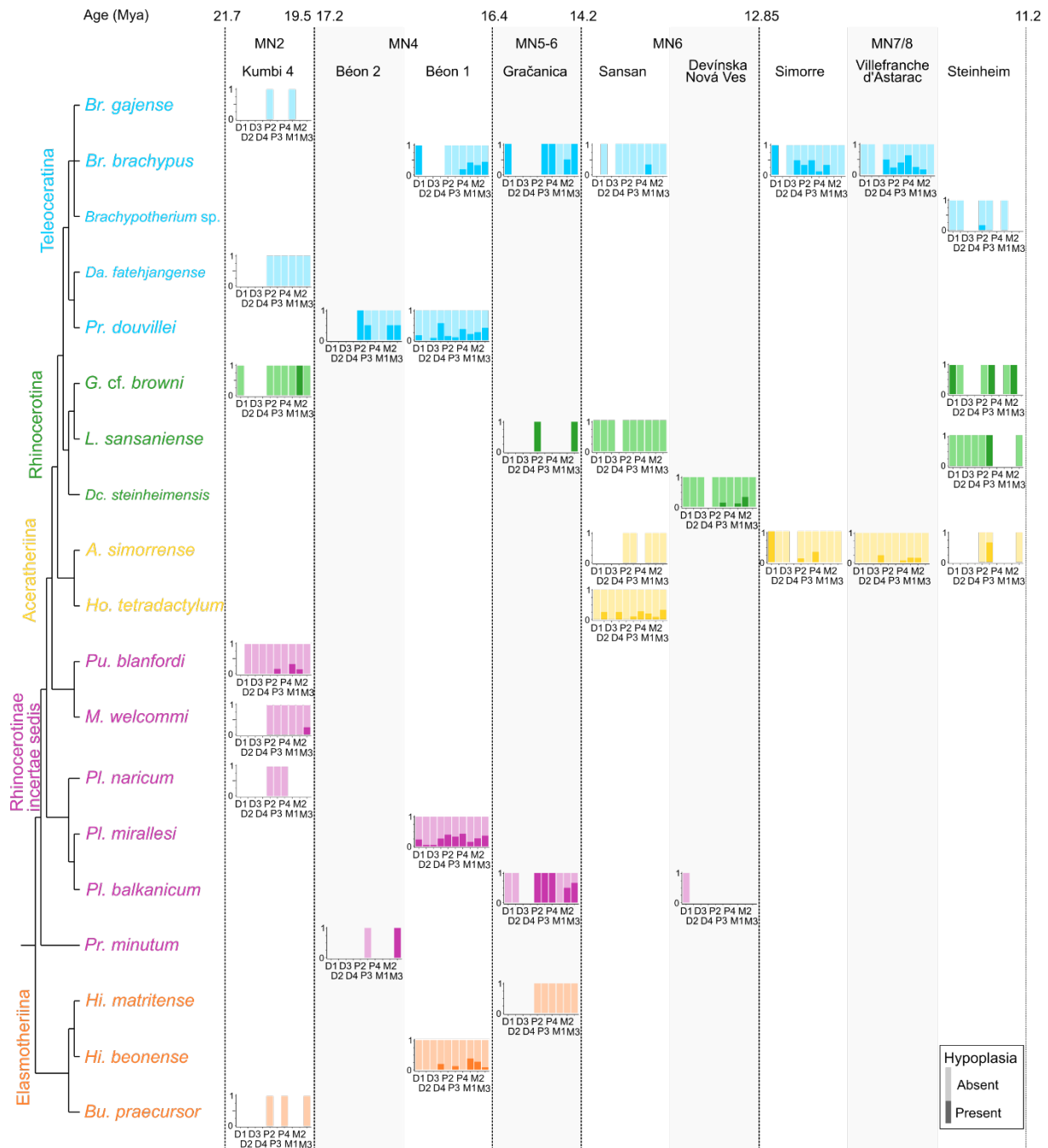


364

365 **Figure 5: Number (A) and Frequency (B) of hypoplasia by Locality and Species**

366 Numbers on barplot A indicate the number of hypoplastic teeth (dark colors) versus unaffected ones
 367 (light colors). Frequencies are calculated as the ratio of hypoplastic teeth on the total number of teeth
 368 (hypoplastic and normal). Sub-tribes colored in blue: Teleoceratina, in green: Rhinocerotina; in yellow:
 369 Aceratheriina, in pink: stem Rhinocerotinae, and in orange: Elasmotheriina
 370 Abbreviations: DNV: Devínska Nová Ves, Sim: Simorre, Vil: Villefranche d'Astarac
 371 Df: *Diaceratherium fatehjangense*, Bg: *Brachypotherium gajense*, Bp: *Bugtirhinus praecursor*, Gb:
 372 *Gaindatherium cf. browni*, Mw: *Mesaceratherium welcommi*, Pbl: *Pleuroceros blanfordi*, Pn:
 373 *Plesiaceratherium naricum*, Pmin: *Protaceratherium minutum*, Pd: *Prosantorhinus douvillei* (*P. aff.*
 374 *douvillei* at Béon 2), Bb: *Brachypotherium brachypus*, Hb: *Hispanotherium beonense*, Pmir:
 375 *Plesiaceratherium mirallesi*, Hm: *Hispanotherium cf. matritense*, Ls: *Lartetotherium sansaniense*, Pba:

376 *Plesiaceratherium balkanicum*, As: *Alicornops simorreense*, Ht: *Hoploaceratherium tetradactylum*, Ds:
 377 *Dicerorhinus steinheimensis*, B: *Brachypotherium* sp.
 378



379
 380 **Figure 6: Prevalence of hypoplasia by locality, species and tooth locus plotted against**
 381 **phylogeny**

382 Phylogenetic relationships follow formal parsimony analyses (Antoine, 2002; Antoine et al., 2010;

383 Becker et al., 2013; Tissier et al., 2020).

384 Subtribes colored in blue: Teleoceratina, in green: Rhinocerotina; in yellow: Aceratheriina, in pink:
 385 stem Rhinocerotinae, and in orange: Elasmotheriina
 386 Dark colors: hypoplastic teeth; Light colors: unaffected teeth

387

388 **Table 4: Prevalence of hypoplasia by locality (number of specimens/percentages)**

	Hypoplastic	Normal	Percentage of hypoplasia
Kumbi 4	93	6	6.06
Béon 2	13	5	27.78
Béon 1	616	216	25.96
Gračanica	16	15	48.39
Devínska Nová Ves	43	5	10.42
Sansan	118	14	10.61
Simorre	60	11	15.49
Villefranche d'Astarac	111	23	17.16
Steinheim	29	7	19.44

389

390

391 Concerning the loci, milk teeth (47/294; 15.99 %) were overall less affected by hypoplasia than
 392 permanent ones (255/1107; 23.04 %; Table 5). Indeed, besides at Béon 1, very few milk molars are
 393 hypoplastic (one D1/d1 at Gračanica and Steinheim, two D1 at Simorre, two D2 and 1 d4 at Sansan, 4
 394 D4/d4 at Villefranche d'Astarac). Upper and lower teeth were equally affected (Kruskal-Wallis, $df = 1$,
 395 p -value = 0.11), with respectively 19.86 % (144/725) and 23.37 % (158/676) of teeth bearing
 396 hypoplasia. The most affected locus was the fourth milk molar with 38.24 % (26/68), while the least
 397 affected were second and third milk molars with around 4 % affected (3/68 and 3/72 respectively;
 398 Table 5). Other loci particularly affected were fourth premolars (60/200; 30 %), third molars (50/188;
 399 26.60 %), and second molars (49/202; 24.26 %; Table 5). Once again, these findings mostly result
 400 from the dominance of Béon 1 specimens in the sample, and great differences in the hypoplasia
 401 pattern are observed by locality (Figure 6). Indeed, if virtually all tooth loci are likely to be affected for
 402 Béon 1 rhinocerotids, the pattern is less varied at other localities although it seemingly diversifies with
 403 sample size (e.g., *H. tetradactylum* from Sansan and Villefranche d'Astarac). For instance, hypoplastic
 404 teeth are nearly exclusively molars at Kumbi 4 (with only one defect on a p3), and permanent teeth at
 405 Gračanica (only one defect on a D1; Figure 6).

406

407 **Table 5: Prevalence of hypoplasia by tooth locus, regardless of provenance and taxon**

408 Upper and lower teeth merged as they have a similar timing of development

	Hypoplastic	Normal	Percentage of hypoplasia
D1	71	15	17.44
D2	65	3	4.41
D3	69	3	4.17
D4	42	26	38.24
Total decidual teeth	47	247	15.99
P2	130	26	16.67
P3	138	33	19.30
P4	140	60	30.00
M1	153	37	19.47
M2	153	49	24.26
M3	138	50	26.60
Total permanent teeth	255	852	23.04

409

410 **GLMM:** For all response variables (Hypo, Defect, Multiple, Localization, and Severity), model support
 411 increased (i.e., lower AIC) when intraspecific factors (e.g., Tooth Loci, Genus, Locality) were included.
 412 When Genus was not forced into the models, the final models contained three to six factors, including
 413 Specimen, the random factor, by default in all models. Defect (converted to a factor) was in the final
 414 models of all concerned variables (Multiple, Localization, and Severity). Genus was in the final models
 415 of all variables but Localization. Position was in the final models of Hypo, Defect, and Localization,
 416 while Tooth, and Wear were in that of Hypo and Defect. Details and comparison of all models can be
 417 seen in electronic supplementary material S5 and S7.

418

419 Based on GLMMs results, we can assess the influence of Genus, Locality, and Tooth on the
 420 hypoplasia pattern. *Alicornops* was less affected than *Brachyotherium* (p-value = 0.015), while
 421 *Plesiaceratherium* was more prone to hypoplasia than *Hispanotherium* (p-value = 0.02). GLMMs
 422 revealed differences in the patterns of hypoplasia (i.e., type of defects and their frequencies) between
 423 *Brachyotherium* and the following taxa: *Dicerorhinus* (p-value = 0.0046), *Alicornops* (p-value <
 424 0.001), and *Protaceratherium* (p-value = 0.034). Tukey's contrasts also revealed the lowest p-values
 425 between *Alicornops* and the following taxa: *Hispanotherium* (p-value = 0.064), *Plesiaceratherium* (p-
 426 value < 0.01), *Prosantorhinus* (p-value < 0.01), *Protaceratherium* (p-value = 0.05). Eventually

427 *Dicerorhinus* had a different hypoplasia pattern than *Plesiaceratherium* (p -value = 0.034) and
428 *Prosantorhinus* (p -value = 0.071).

429

430 Concerning tooth loci, all teeth but fourth premolars and third molars are less affected than fourth milk
431 molars (p -values < 0.05). The results further suggested that the most commonly affected loci were
432 third molars, fourth premolars and fourth milk molars, while the least affected were all milk molars but
433 the fourth. Concerning localities, Gračanica teeth were significantly more touched than Béon 1 and
434 Sansan specimens (p -values \approx 0.01). Middle Miocene rhinocerotids present a hypoplasia pattern
435 distinct from that of early Miocene ones (p -value = 0.019). Similarly to GLMMs for DMTA, we observed
436 confounding effects. Slightly-worn teeth had less hypoplasia than average worn (p -value = 0.005) and
437 very worn teeth (p -value = 0.026).

438

439 **Discussion**

440

441 Dietary preferences and niche partitioning of the rhinocerotids studied

442 The comparison of the fossil specimens DMT to that of extant ones highlighted important differences.
443 This suggests that the dietary spectrum of extinct rhinocerotids might have been very distinct from that
444 observed in the living species (Hullot et al., 2019). However, the microwear textures of the fossils are
445 critically distinct from that of the only extant strict grazer *Ceratotherium simum*, banning such dietary
446 preferences for the studied fossil specimens. This finding is not surprising as grasses and associated
447 grazing ungulates expended only during latest Miocene in Eurasia (Janis, 2008). The reconstructed
448 dietary preferences based on DMTA are presented in Table 6 by locality and by species.

449

450 The DMTA results of fossil specimens on both facets (Figure 3; Figure 4) suggest a clear niche
451 partitioning based on feeding preferences for the rhinocerotid specimens studied at Kumbi 4, Sansan,
452 and Villefranche d'Astarac. Although DMT could only be explored in four out of the nine rhinocerotid
453 species present at Kumbi 4, the patterns observed indicate clear differences in the feeding behaviors,
454 even if leaf consumption seems to be a major component for all rhinocerotids studied but *B. gajense*.

455

456 **Table 6: Dietary preferences inferred from textural microwear (DMTA) of the studied**
 457 **rhinocerotid specimens from different fossil localities of the lower and middle Miocene of**
 458 **Eurasia.**

459 Color code: brown/B – browser, blue/M – mixed-feeder, light green/F – folivore, no color/x – not
 460 studied

	Kumbi 4	Béon 2	Béon 1	Gračanica	Sansan	Devínska Nová Ves Spalte	Simorre	Villefranche d' Astarac	Steinheim am Albuch
Rhinocerotinae									
<i>Mesaceratherium welcommi</i>	M								
<i>Pleuroceros blanfordi</i>	M								
<i>Protaceratherium</i> sp.	x								
<i>Protaceratherium minutum</i>		x							
<i>Plesiaceratherium naricum</i>	x								
<i>Plesiaceratherium mirallesi</i>		x	F						
<i>Plesiaceratherium balkanicum</i>				F		B			
<i>Plesiaceratherium</i> sp.									
<i>Hoploaceratherium tetradactylum</i>					B				
<i>Alicornops simorreense</i>					M		x	F	M
<i>Gaindatherium</i> cf. <i>browni</i>	M								
<i>Lartetotherium sansaniense</i>				B	B				x
<i>Dicerorhinus steinheimensis</i>						B			x
<i>Diaceratherium fatehjangense</i>	x								
<i>Brachypotherium gajense</i>	B								
<i>Brachypotherium brachypus</i>			M	F	M		B	B	
<i>Brachypotherium</i> sp.									x
<i>Prosantorhinus shahbazi</i>	x								
<i>Prosantorhinus douvillei</i>		aff.	B						
Elasmotheriinae									
<i>Bugtirhinus praecursor</i>	x								
<i>Hispanotherium beonense</i>			M						
<i>Hispanotherium</i> cf. <i>matritense</i>				M					

461

462

463 This finding is in line with the inferred lush vegetation under warm and moist climatic conditions

464 proposed for this locality, providing abundant and diverse feeding resources for the many large

465 herbivores present (Antoine et al., 2010, 2013; Martin et al., 2011). The dietary preferences

466 reconstructed for Sansan rhinocerotids suggest the co-occurrence of two browsers (*L. sansaniense*

467 and *H. tetradactylum*, the latter including harder items in its diet) and two mixed-feeders (*A.*

468 *simorreense* and *B. brachypus*), coherent with the (sub-)tropical forested environment reconstructed for

469 that locality (Costeur et al., 2012), but at odds with the recent-like Miocene coolhouse as depicted by

470 Westerhold et al. (2020; ~415 parts per million CO₂). This niche partitioning is probably accentuated

471 by different habitat preferences: *H. tetradactylum* is mostly found in swamp or fluvial sediments

472 indicating wet habitat preferences contrary to *A. simorreense*, while *B. brachypus* seems intermediate
473 and *L. sansaniense* generalist (Heissig, 2012). Eventually, we observed obvious differences in the
474 dietary preferences for *A. simorreense* (folivore or mixed-feeder favoring leaves) and *B. brachypus*
475 (browser including hard objects) at Villefranche d'Astarac, where a humid forested environment is
476 hypothesized (Bentaleb et al., 2006).

477

478 On the contrary, an overlap of microwear textures, especially for the grinding facet, is observed for the
479 localities of Béon 1 and Gračanica. Besides diet, different habitats and feeding heights might result in
480 niche partitioning (Hutchinson, 1959; Arsenault and Owen-Smith, 2008). Concerning Béon 1, a partial
481 niche partitioning due to habitat differences has been hypothesized for the rhinocerotids – swamps for
482 both teleoceratines *B. brachypus* and *P. douvillei*, open woodland for *P. mirallesi*, and savannah-like
483 open environments for *H. beonense* (Bentaleb et al., 2006) – and subtle dietary differences are
484 discussed in Hullot et al. (2021) in the light of the combination of molar mesowear and dental
485 microwear texture analysis. At Gračanica, 2D microwear and mesowear score already revealed an
486 overlap in the dietary preferences of *Pl. balkanicum* and *B. brachypus* as two browsing species,
487 although the latter is labelled as “dirty browsing”, a dietary category (not defined by comparative
488 datasets on intensively studied extant species with known diets) including species assumed to browse
489 and incorporate soil particles. (Xafis et al., 2020). Although microwear sampling is restricted and
490 includes premolars for the other two rhinocerotids (*L. sansaniense* and *H. cf. matritense*), it points
491 towards different mixed-feeding behaviors, most likely with a dominance of grass in the diet of *H. cf.*
492 *matritense* (Xafis et al., 2020). The very low values of complexity for all Gračanica rhinocerotids in our
493 sample, combined to relatively high values of anisotropy (Figure 3; Figure 4), could suggest an
494 important consumption of leaves for all species, as well as a very low amount of lignified tissues that
495 would have required more grinding to get access to cell content. Interestingly, the reconstructed
496 environment at this locality (based on mammal assemblage and flora) is a lowland swamp surrounded
497 by a closed canopy-like environment (Butzmann et al., 2020; Xafis et al., 2020), meaning that leaves
498 would have been an abundant resource. This recalls the feeding preferences and microwear textures
499 of the extant *Dicerorhinus sumatrensis* (Sumatran rhino; Hullot et al., 2019). Eventually, the restricted
500 DMTA samples from Devínska Nová Ves Spalte, Steinheim am Albuch, and Simorre suggest browsing

501 or mixed-feeding habits for all specimens studied, but did not allow to conclude on potential
502 competition for food resources.

503

504 Interactions with co-occurring herbivores

505 Besides other rhinocerotid species, the individuals studied co-occurred with many other herbivore
506 mammals. Although co-occurrence is not necessarily a good proxy for ecological interactions
507 (Blanchet et al., 2020), it is possible that some of these herbivores were competing for or partitioning
508 food resources with the rhinocerotids. Unfortunately, very little has been studied concerning the dietary
509 preferences of the fauna at most of the studied localities with the notable exceptions of Gračanica and
510 Sansan.

511

512 Indeed, recent studies on dental wear (micro- and meso- wear) or stable isotopy, suggested frugivory
513 for some associated species such as tragulids (*Dorcatherium* spp. at all localities but Simorre and
514 Villefranche; Aiglstorfer et al., 2014; Xafis et al., 2020), the middle Miocene Moschidae (*Micromeryx*
515 spp. found at Sansan, Simorre and Steinheim am Albuch; Aiglstorfer and Semperebon, 2019) or the
516 chalicothere *Metaschizotherium fraasi* (found at Steinheim am Albuch; Semperebon et al., 2011).
517 Interestingly, no rhinocerotid specimens studied here seemingly favored fruits. Similarly, the lophodont
518 suid *Listriodon splendens*, found at Gračanica, Devínska Nová Ves, and Simorre, might have favored
519 grasses (Van der Made, 2003; Xafis et al., 2020), a resource not exploited by the rhinocerotids either.
520 Otherwise, the vast majority of herbivore species were probably browsers or mixed-feeders, in good
521 agreement with the statement by Eronen and Rössner (2007) that these forms were dominant
522 between MN4 and MN9. This is for instance the case of the associated perissodactyl species
523 *Anisodon grande* (Chalicotheriidae), which 2D microwear signal at Devínska Nová Ves suggests
524 folivory (Semperebon et al., 2011), and *Anchitherium* spp. (Equidae) ranging from generalists to “dirty
525 browsers” (Kaiser, 2009; Xafis et al., 2020).

526

527 Within browsers and mixed-feeders, resources partitioning is still possible (e.g., consumption of
528 different plant parts or species) but might be difficult to detect in fossil communities. Moreover, other
529 strategies can lead to niche partitioning, such as different habitat, different body mass, or different
530 feeding height (Hutchinson, 1959; Schoener, 1974; Arsenault and Owen-Smith, 2008). Regarding
531 body mass, most rhinocerotids studied are megaherbivores *sensu* Owen-Smith (1988; terrestrial

532 herbivores weighting more than 1000 kg), which implies specific feeding strategies and metabolic
533 requirements. Megaherbivores are often treated as a separate herbivore guild, mostly disturbing that
534 of mesoherbivores (4–450 kg ; Fritz et al., 2002; Calandra et al., 2008; Landman et al., 2013). Within
535 megaherbivores, proboscideans frequently co-occurred with rhinocerotids at the studied localities and
536 were mostly browsers or mixed-feeders, placing them as direct competitors for rhinocerotids. Indeed,
537 the mesowear and 2D microwear suggest that *Prodeinotherium bavaricum* and *Gomphotherium*
538 *angustidens* were browsers at Gračanica (Xafis et al. 2020), while the mesowear angle categorizes *P.*
539 *bavaricum* from Sansan, *D. giganteum* from Villefranche d’Astarac and *G. angustidens* from Simorre
540 as browsers, but *G. angustidens* from Sansan and Villefranche d’Astarac as mixed-feeders (Loponen,
541 2020). Such overlapping in the diet of proboscideans and rhinocerotids is observed nowadays
542 between African elephants and black rhinoceroses (Landman et al., 2013). Interestingly, this
543 competition is detrimental to the rhinoceros, whose individuals shift towards the inclusion of more
544 grasses in presence of elephants (on a seasonal basis). Another possibility, as postulated by Xafis et
545 al. (2020) for *Deinotherium* spp. and *Plesiaceratherium balkanicum* at Gračanica, would be different
546 feeding heights between proboscideans and rhinocerotids, as the first ones were most likely feeding at
547 the top of trees due to their larger size (some of the biggest Neogene mammals; Larramendi, 2015).

548

549 Hypoplasia prevalence and environmental conditions

550 We found that the hypoplasia prevalence and pattern (i.e., tooth loci affected) were very different
551 depending on the locality and the species concerned. Except for Kumbi 4, the prevalence was
552 relatively high (> 10 %) at all sites of our early-middle Miocene sample. Even though nine species of
553 rhinocerotids are found at Kumbi 4, such a low prevalence is in agreement with previous results in the
554 region over the Cenozoic (Roohi et al., 2015), and coherent with the very favorable, low-stress context
555 hypothesized at this locality, that is a rich vegetation under a warm and humid climate (Antoine et al.,
556 2013).

557

558 The prevalence of hypoplasia is high at Béon 1 (>25 %) for all rhinocerotids except *H. beonense*, with
559 molars being particularly affected with respect to other dental loci. Second and third molars are the last
560 teeth to develop and erupt in rhinocerotids (Hitchins, 1978; Hillman-Smith et al., 1986; Böhmer et al.,
561 2016), and stresses on these late-developed teeth have been correlated with environmental, seasonal

562 stresses in sheep (Upex and Dobney, 2012). Although subtropical wet conditions are reconstructed at
563 Béon 1 (just prior to the MCO), periodic droughts are also reported in the area at that time (Duranthon
564 et al., 1999; Hullot and Antoine, 2020). Interestingly, the least affected species is the elasmotheriine *H.*
565 *beonense*, an early representative of a clade adapted to relatively open and arid environments
566 (Cerdeño and Nieto, 1995; Iñigo and Cerdeño, 1997), and which displays a mixed-feeding diet (Figure
567 4). On the contrary, both teleoceratine species, often considered swamp dwellers, display a high
568 prevalence of hypoplasia (Figure 5).

569
570 We found a very high prevalence of hypoplasia at Gračanica, with nearly 50 % of the teeth bearing at
571 least one hypoplastic defect. The proposed age for the locality ranges between 14.8 and 13.8 Ma
572 (Göhlich and Mandic, 2020), which is an interval of great climatic changes. Indeed, though included in
573 the MCO, the interval from 14.7 to 14.5 Ma present an increased seasonality in precipitations, with
574 prolonged dry periods (Böhme, 2003). On the other hand, an abrupt cooling occurred between 14 and
575 13.5 Ma, correlating with the Mi-3 event (Zachos et al., 2001; Böhme, 2003; Holbourn et al., 2014;
576 mMCT of Westerhold et al., 2020). Besides this challenging environmental context for the
577 rhinocerotids, our DMTA results suggest a potential competition for food resources (Figure 3), that
578 could have generated stressful conditions.

579
580 At Sansan, the prevalence of hypoplasia is overall moderate (~ 10 %) and defects are only found in
581 two species out of four: *H. tetradactylum* and *B. brachypus* (only one M1). The pattern of hypoplasia
582 for *H. tetradactylum*, with various loci affected, suggests different stresses and timing, from *in utero*
583 (D2) to post-weaning (M3). It is quite remarkable, as the proximity of the MCO peak (Maridet and Sen,
584 2012) leading to seasonal warm and moist conditions (Costeur et al., 2012), would seemingly
585 constitute relatively low stress conditions for the concerned rhinocerotids.

586
587 The prevalence of hypoplasia at Devínska Nová Ves Spalte is also moderate (5/48; 10.42 %) and
588 restricted to *D. steinheimensis* (P3, M1, M2 only; Figure 6), although the locality dates from the
589 mMCT. However, despite this transitional climatic system, pollen data from the Vienna Basin, to which
590 the locality belongs, indicate that regional conditions remained tropical with few precipitation variations
591 (Sabol and Kováč, 2006), coherent with the absence of hypoplasia on third molars, that can be

592 correlated with seasonal stresses. The paleogeographic context seems to have played a major role,
593 as the taxonomic differences with Sansan are partly explained by different paleoenvironments:
594 Devínska Nová Ves Spalte was a forested area near the shoreline of the transgressive late Langhian
595 sea (Sabol and Kováč, 2006).

596

597 The rhinocerotids from the localities of the MN7/8 (Simorre, Villefranche d'Astarac, and Steinheim am
598 Albuch), a time of sea-level drop and comparatively dry climate (Legendre et al., 2005; Böhme et al.,
599 2011; Heissig, 2012; Westerhold et al., 2020), present higher prevalences but contrasted patterns
600 depending on the species and locality (Figure 5; Figure 6). However, contrary to what we could have
601 been expected regarding the environmental conditions, the most affected loci (P2, P3, D1) document
602 mostly early-life stresses (e.g., birth, juvenile disease), rather than environmental or seasonal stresses
603 (Niven et al., 2004; Upex and Dobney, 2012). At Steinheim, only *L. sansaniense* has hypoplasia on
604 other teeth than second and third premolars, suggesting mostly early life stresses. At Simorre, more
605 loci are affected (D1, P2-P3, P4, and M1) and the pattern is relatively similar for both co-occurring
606 species i.e., *B. brachypus* and *A. simorreense*. Hypoplasia on D1, that develops mostly *in utero*
607 synchronously with D4, could indicate birth-related stresses (Hillman-Smith et al., 1986; Mead, 1999;
608 Böhmer et al., 2016). Similarly, the M1 starts its development relatively early, attested by the presence
609 of a neonatal line in some rhinocerotid teeth (Tafforeau et al., 2007), revealing particularly stressful
610 conditions around birth. Eventually, the rhinocerotids from Villefranche d'Astarac document later-life
611 stresses, with hypoplasia recorded from D4 to M2 (not P2-P3 for *A. simorreense*). The fourth premolars
612 are particularly affected in *B. brachypus*, which could indicate harsh weaning or cow-calf separation
613 conditions.

614

615 Paleoecologic implications and changes

616 Several species or genera are retrieved in various localities overtime, but *B. brachypus* clearly has the
617 longest range (from Béon 1 [MN4] to Simorre + Villefranche d'Astarac [MN7/8], with Gračanica [MN5-
618 6] and Sansan [MN6] in the meantime). We observe a clear shift in the DMT of *B. brachypus* over time
619 from a mixed-feeding behavior at Béon 1, Gračanica, and Sansan to a clear browsing signal with the
620 ingestion of harder items (fruits, seeds, or even soil) at Simorre and Villefranche d'Astarac (Figure 3;
621 Figure 4). This result could be due to a change in the regional climatic conditions, from warm and

622 humid pre-MCO to cooler, more seasonal and arid post-MCO (Zachos et al., 2001; Böhme, 2003;
623 Holbourn et al., 2014), perhaps leading to behavioral changes in this species (Cerdeño and Nieto,
624 1995), and/or to changes in local conditions.

625

626 Contrastingly, the DMT of *A. simorreense* remains quite similar from Sansan (MN6) to Steinheim
627 (MN7/8; Figure 3; Figure 4). Interestingly, there are clear differences in the hypoplasia prevalence of
628 these two species, *B. brachypus* being one of the most affected species in our sample. Such
629 differences in the hypoplasia prevalence could reveal the existence of a competition for food and/or
630 water resources. The pattern of hypoplasia at Simorre (D1, P2-P3) and Villefranche d'Astarac (D4-M1,
631 P4-M2) suggests early life stresses for both rhinocerotids (Figure 6), mostly before weaning (Mead,
632 1999).

633

634 Concerning other species found at more than one locality (*L. sansaniense*, *D. steinheimhensis*, and
635 *Plesiaceratherium* spp.), the hypoplasia patterns seem to be different at each locality, denoting a
636 greater effect of local conditions than species-related sensitivities. Only the *Plesiaceratherium* species
637 from Béon 1 and Gračanica exhibit comparable patterns (Figure 6), although it could be related to the
638 high prevalence of stresses for individuals belonging to the concerned taxa at these localities. Overall,
639 the elasmotheriines (*Bugtirhinus* and *Hispanotherium*) were seemingly spared by hypoplasia. Indeed,
640 no tooth was hypoplastic at Kumbi 4 (*B. praecursor*; 0/4) and Gračanica (*H. cf. matritense*; 0/6). At
641 Béon 1, for which a greater sample is available, *H. beonense* is the least affected species with 13.04
642 % (12/92) of hypoplastic teeth, nearly exclusively permanent (only one hypoplasia on a D4). If this
643 result was not surprising at Kumbi 4, where low-stress conditions were inferred and very little
644 hypoplasia recorded for all studied species, the difference to other associated species was particularly
645 striking at Béon 1 and Gračanica. The microwear study of elasmotheriines is restricted in the literature,
646 but it suggests the inclusion of a non-negligible part of browse resources in the diet, at least
647 seasonally (Rivals et al., 2020; Xafis et al., 2020). This finding is in line with our DMTA results for
648 *Hispanotherium* species (Béon 1 and Gračanica) suggesting mixed-feeding preferences (Figure 3;
649 Figure 4). The increasing crown height observed in this clade over time could allow for
650 accommodating to a greater variety of food items (Semperebon and Rivals, 2007; Damuth and Janis,
651 2011; Tütken et al., 2013), thus limiting nutritional stress, as observed in hipparionine equids, with

652 respect to anchitheriine equids (MacFadden, 1992; Janis, 2008; Muhlbachler et al., 2011). The classic
653 view of elasmotheriines as obligate open-environment rhinocerotids adapted to grazing – notably
654 based on representatives from the arid Iberic Peninsula (Iñigo and Cerdeño, 1997) – is thus somehow
655 challenged. This could mean that hypsodonty in this clade might counterbalance significant grit load
656 induced by feeding low in open environments, thus reflecting more the habitat rather than the diet, an
657 hypothesis that has already been proposed to explain hypsodonty evolution (Janis, 1988; Jardine et
658 al., 2012; Semprebon et al., 2019).

659

660 **Conclusions**

661

662 The study of the paleoecology of rhinocerotids from the early and middle Miocene of Eurasia revealed
663 clear differences over time and space between or within species. Though, DMTA results suggested
664 only browsers and mixed-feeders (no grazers nor frugivores) in the studied rhinocerotid sample, they
665 unraveled clear niche partitioning through food resources at several diachronous localities (Kumbi 4,
666 Sansan, and Villefranche d'Astarac). At other localities (Béon 1, Gračanica), a significant overlap of
667 microwear textures was observed, and more subtle differences in food preferences and other niche
668 partitioning strategies (habitat, feeding height) may have existed. Regarding enamel hypoplasia, which
669 is quite prevalent in the studied sample (except in the oldest and only South Asian locality, Kumbi 4), it
670 revealed clear disparities between localities, species, and dental loci. While the effects of climate
671 changes were not immediately obvious, we discussed more specific, local conditions that may explain
672 the observed stresses. Regarding a potential phylogenetic effect, we were able to highlight very
673 different sensitivities: while *B. brachypus* is highly affected by hypoplasia regardless of locality and
674 conditions, elasmotheriines (*Bugtirhinus praecursor* at Kumbi 4, *Hispanotherium beonense* at Béon 1
675 and *H. cf. matritense* at Gračanica) are pretty spared in contrast. Over time and depending on the
676 conditions, differences in DMT and/or prevalence of hypoplasia were observed for some species found
677 in several localities. This is notably the case for the feeding preferences of *B. brachypus*, oscillating
678 between browser and mixed feeder, or for the hypoplasia profiles of *L. sansaniense* and *D.*
679 *steinheimensis* denoting different stress periods and local conditions.

680

681

682 **Acknowledgments**

683

684 The sampling for this study was partly funded by SYNTHESYS AT-TAF-65 (2020; Naturhistorisches
685 Museum Wien, Austria) and a Bourse de Mobilité Doctorale from the Association Française des
686 Femmes Diplômées des Universités. We are indebted to the curators in charge of all the collections
687 we visited and studied: U. Göhlich (NHMW), L. Costeur (NHMB), Y. Laurent and P. Dalous (MHNT).

688

689

690 **References**

691

692 Aiglstorfer, M., and G. M. Semprebon. 2019. Hungry for fruit? – A case study on the ecology of middle
693 Miocene Moschidae (Mammalia, Ruminantia). *Geodiversitas*, 41:385–399. doi:
694 10.5252/geodiversitas2019v41a10.

695 Aiglstorfer, M., G. E. Rössner, and M. Böhme. 2014. *Dorcatherium nauai* and pecoran ruminants from the late
696 Middle Miocene Gratkorn locality (Austria). *Palaeobiodiversity and Palaeoenvironments*, 94:83–123.

697 Antoine, P.-O. 2002. Phylogénie et évolution des Elasmotheriina (Mammalia, Rhinocerotidae). *Mémoires Du*
698 *Muséum National d’Histoire Naturelle*, 188:5–350.

699 Antoine, P.-O. in press. Rhinocerotids from the Siwalik faunal sequence; p. *In* C. Badgley, D. Pilbeam, and M.
700 Morgan (eds.), *At the Foot of the Himalayas: Paleontology and Ecosystem Dynamics of the Siwalik*
701 *Record of Pakistan.*, Johns Hopkins University Press.

702 Antoine, P.-O., and F. Duranthon. 1997. Découverte de *Protaceratherium minutum* (Mammalia, Rhinocerotidae)
703 dans le gisement Orléanien (MN 4) de Montréal-du-Gers (Gers). *Annales de Paléontologie (Vert.-*
704 *Invert.)*, 83:201–213.

705 Antoine, P.-O., and J.-L. Welcomme. 2000. A New Rhinoceros From The Lower Miocene Of The Bugti Hills,
706 Baluchistan, Pakistan: The Earliest Elasmotheriine. *Palaeontology*, 43:795–816. doi: 10.1111/1475-
707 4983.00150.

708 Antoine, P.-O., and D. Becker. 2013. A brief review of Agenian rhinocerotids in Western Europe. *Swiss Journal*
709 *of Geosciences*, 106:135–146. doi: 10.1007/s00015-013-0126-8.

710 Antoine, P.-O., F. Duranthon, and P. Tassy. 1997. L’apport des grands mammifères (Rhinocérotidés, Suoidés,
711 Proboscidiens) à la connaissance des gisements du Miocène d’Aquitaine (France). *BoiChro’M97*,
712 spécial 21:581–590.

713 Antoine, P.-O., K. F. Downing, J.-Y. Crochet, F. Duranthon, L. J. Flynn, L. Marivaux, G. Métais, A. R. Rajpar,
714 and G. Roohi. 2010. A revision of *Aceratherium blanfordi* Lydekker, 1884 (Mammalia:
715 Rhinocerotidae) from the Early Miocene of Pakistan: postcranials as a key. *Zoological Journal of the*
716 *Linnean Society*, 160:139–194. doi: 10.1111/j.1096-3642.2009.00597.x.

717 Antoine, P.-O., G. Métais, M. Orliac, J. Crochet, L. Flynn, L. Marivaux, A. Rajpar, Dr. G. Roohi, and J.
718 Welcomme. 2013. Mammalian Neogene biostratigraphy of the Sulaiman Province, Pakistan; p. 400–
719 422. *In* *Fossil Mammals of Asia: Neogene Biostratigraphy and Chronology*. Columbia University Press
720 doi: 10.13140/2.1.3584.5129.

721 Arman, S. D., T. A. A. Prowse, A. M. C. Couzens, P. S. Ungar, and G. J. Prideaux. 2019. Incorporating

- 722 intraspecific variation into dental microwear texture analysis. *Journal of The Royal Society Interface*,
723 16:20180957. doi: 10.1098/rsif.2018.0957.
- 724 Arsenault, R., and N. Owen-Smith. 2008. Resource partitioning by grass height among grazing ungulates does
725 not follow body size relation. *Oikos*, 117:1711–1717. doi: [https://doi.org/10.1111/j.1600-](https://doi.org/10.1111/j.1600-0706.2008.16575.x)
726 0706.2008.16575.x.
- 727 Bates, D., M. Mächler, B. Bolker, and S. Walker. 2015. Fitting linear mixed-effects models using lme4. *Journal*
728 *of Statistical Software*, 67:1–48. doi: doi:10.18637/jss.v067.i01.
- 729 Becker, D., and J. Tissier. 2020. Rhinocerotidae from the early middle Miocene locality Gračanica (Bugojno
730 Basin, Bosnia-Herzegovina). *Palaeobiodiversity and Palaeoenvironments*, 100:395–412. doi:
731 10.1007/s12549-018-0352-1.
- 732 Becker, D., P.-O. Antoine, and O. Maridet. 2013. A new genus of Rhinocerotidae (Mammalia, Perissodactyla)
733 from the Oligocene of Europe. *ResearchGate*, 2013:947–972. doi: 10.1080/14772019.2012.699007.
- 734 Bentaleb, I., C. Langlois, C. Martin, P. Iacumin, M. Carré, P.-O. Antoine, F. Duranthon, I. Moussa, J.-J. Jaeger,
735 and N. Barrett. 2006. Rhinocerotid tooth enamel 18O/16O variability between 23 and 12 Ma in
736 southwestern France. *Comptes Rendus Geoscience*, 338:172–179. doi: 10.1016/j.crte.2005.11.007.
- 737 Berlioz, É., D. S. Kostopoulos, C. Blondel, and G. Merceron. 2018. Feeding ecology of *Eucladoceros ctenoides*
738 as a proxy to track regional environmental variations in Europe during the early Pleistocene. *Comptes*
739 *Rendus Palevol*, 17:320–332. doi: 10.1016/j.crpv.2017.07.002.
- 740 Blanchet, F. G., K. Cazelles, and D. Gravel. 2020. Co-occurrence is not evidence of ecological interactions.
741 *Ecology Letters*, 23:1050–1063. doi: 10.1111/ele.13525.
- 742 Böhme, M. 2003. The Miocene Climatic Optimum: evidence from ectothermic vertebrates of Central Europe.
743 *Palaeogeography, Palaeoclimatology, Palaeoecology*, 195:389–401. doi: 10.1016/S0031-
744 0182(03)00367-5.
- 745 Böhme, M., A. Ilg, and M. Winklhofer. 2008. Late Miocene “washhouse” climate in Europe. *Earth and Planetary*
746 *Science Letters*, 275:393–401. doi: 10.1016/j.epsl.2008.09.011.
- 747 Böhme, M., M. Winklhofer, and A. Ilg. 2011. Miocene precipitation in Europe: Temporal trends and spatial
748 gradients. *Palaeogeography, Palaeoclimatology, Palaeoecology*, 304:212–218.
- 749 Böhmer, C., K. Heissig, and G. E. Rössner. 2016. Dental Eruption Series and Replacement Pattern in Miocene
750 *Prosantorhinus* (Rhinocerotidae) as Revealed by Macroscopy and X-ray: Implications for Ontogeny
751 and Mortality Profile. *Journal of Mammalian Evolution*, 23:265–279. doi: 10.1007/s10914-015-9313-x.
- 752 Bruch, A. A., D. Uhl, and V. Mosbrugger. 2007. Miocene climate in Europe — Patterns and evolution: A first
753 synthesis of NECLIME. *Palaeogeography, Palaeoclimatology, Palaeoecology*, 253:1–7. doi:
754 10.1016/j.palaeo.2007.03.030.
- 755 Butzmann, R., U. B. Göhlich, B. Bassler, and M. Krings. 2020. Macroflora and charophyte gyrogonites from the
756 middle Miocene Gračanica deposits in central Bosnia and Herzegovina. *Palaeobiodiversity and*
757 *Palaeoenvironments*, 100:479–491. doi: 10.1007/s12549-018-0356-x.
- 758 Calandra, I., U. B. Göhlich, and G. Merceron. 2008. How could sympatric megaherbivores coexist? Example of
759 niche partitioning within a proboscidean community from the Miocene of Europe. *Die*
760 *Naturwissenschaften*, 95:831–838. doi: 10.1007/s00114-008-0391-y.
- 761 Cerdeño, E. 1998. Diversity and evolutionary trends of the Family Rhinocerotidae (Perissodactyla).
762 *Palaeogeography, Palaeoclimatology, Palaeoecology*, 141:13–34. doi: [https://doi.org/10.1016/S0031-](https://doi.org/10.1016/S0031-0182(98)00003-0)
763 0182(98)00003-0.
- 764 Cerdeño, E., and M. Nieto. 1995. Changes in Western European Rhinocerotidae related to climatic variations.
765 *Palaeogeography, Palaeoclimatology, Palaeoecology*, 114:325–338.

- 766 Cerling, T. E., J. M. Harris, B. J. MacFadden, M. G. Leakey, J. Quade, V. Eisenmann, and J. R. Ehleringer.
767 1997. Global vegetation change through the Miocene/Pliocene boundary. *Nature*, 389:153–158.
- 768 Costeur, L., C. Guérin, and O. Maridet. 2012. Paléoécologie et paléoenvironnement du site miocène de Sansan;
769 p. 661–693. In S. Peigné and S. Sen (eds.), *Mammifères de Sansan*, Mémoires du Muséum national
770 d’Histoire naturelle. Vol. 203. Paris.
- 771 Damuth, J., and C. M. Janis. 2011. On the relationship between hypsodonty and feeding ecology in ungulate
772 mammals, and its utility in palaeoecology. *Biological Reviews*, 86:733–758. doi:
773 <https://doi.org/10.1111/j.1469-185X.2011.00176.x>.
- 774 Duranthon, F., P. O. Antoine, C. Bulot, and J. P. Capdeville. 1999. Le Miocène inférieur et moyen continental du
775 bassin d’Aquitaine Livret-guide de l’excursion des Journées Crouzel (10 et 11 juillet 1999). *Bulletin de*
776 *La Société d’histoire Naturelle de Toulouse*, 135:79–91.
- 777 Eronen, J. T., and G. E. Rössner. 2007. Wetland paradise lost: Miocene community dynamics in large
778 herbivorous mammals from the German Molasse Basin. *Evolutionary Ecology Research*, 9:471–494.
- 779 Fédération Dentaire Internationale. 1982. An epidemiological index of development defects of dental enamel
780 (DDE index). *International Dental Journal*, 42:411–426.
- 781 Fox, J., S. Weisberg, D. Adler, D. Bates, G. Baud-Bovy, S. Ellison, D. Firth, M. Friendly, G. Gorjanc, and S.
782 Graves. 2012. Package ‘car.’ Vienna: R Foundation for Statistical Computing,.
- 783 Fritz, H., P. Duncan, I. J. Gordon, and A. W. Illius. 2002. Megaherbivores influence trophic guilds structure in
784 African ungulate communities. *Oecologia*, 131:620–625.
- 785 Giaourtsakis, I., G. Theodorou, S. Roussiakis, A. Athanassiou, and G. Iliopoulos. 2006. Late Miocene horned
786 rhinoceroses (Rhinocerotinae, Mammalia) from Kerassia (Euboea, Greece). *Neues Jahrbuch Für*
787 *Geologie Und Paläontologie - Abhandlungen*, 239:367–398. doi: 10.1127/njgpa/239/2006/367.
- 788 Göhlich, U. B., and O. Mandic. 2020. Introduction to the special issue “The drowning swamp of Gračanica
789 (Bosnia-Herzegovina)—a diversity hotspot from the middle Miocene in the Bugojno Basin.”
790 *Palaeobiodiversity and Palaeoenvironments*, 100:281–293. doi: 10.1007/s12549-020-00437-0.
- 791 Goodman, A. H., and J. C. Rose. 1990. Assessment of systemic physiological perturbations from dental enamel
792 hypoplasias and associated histological structures. *American Journal of Physical Anthropology*, 33:59–
793 110. doi: 10.1002/ajpa.1330330506.
- 794 Grine, F. E. 1986. Dental evidence for dietary differences in *Australopithecus* and *Paranthropus*: a quantitative
795 analysis of permanent molar microwear. *Journal of Human Evolution*, 15:783–822.
- 796 Heissig, K. 2012. Les Rhinocerotidae (Perissodactyla) de Sansan; p. 317–485. In S. Peigné and S. Sen (eds.),
797 *Mammifères de Sansan*. Vol. 203. Mémoires du Muséum national d’Histoire naturelle, Paris.
- 798 Hillman-Smith, A. K. K., N. R. Owen-Smith, J. L. Anderson, A. J. Hall-Martin, and J. P. Selaladi. 1986. Age
799 estimation of the white rhinoceros (*Ceratotherium simum*). *Journal of Zoology*, 210:355–377.
- 800 Hitchins, P. M. 1978. Age determination of the black rhinoceros (*Diceros bicornis* Linn.) in Zululand. *South*
801 *African Journal of Wildlife Research*, 8:71–80.
- 802 Hoffman, J. M., D. Fraser, and M. T. Clementz. 2015. Controlled feeding trials with ungulates: a new application
803 of in vivo dental molding to assess the abrasive factors of microwear. *The Journal of Experimental*
804 *Biology*, 218:1538–1547. doi: 10.1242/jeb.118406.
- 805 Holbourn, A., W. Kuhnt, M. Lyle, L. Schneider, O. Romero, and N. Andersen. 2014. Middle Miocene climate
806 cooling linked to intensification of eastern equatorial Pacific upwelling. *Geology*, 42:19–22.
- 807 Hullot, M., and P.-O. Antoine. 2020. Mortality curves and population structures of late early Miocene
808 Rhinocerotidae (Mammalia, Perissodactyla) remains from the Béon 1 locality of Montréal-du-Gers,

- 809 France. *Palaeogeography, Palaeoclimatology, Palaeoecology*, 558:109938. doi:
810 10.1016/j.palaeo.2020.109938.
- 811 Hullot, M., P.-O. Antoine, M. Ballatore, and G. Merceron. 2019. Dental microwear textures and dietary
812 preferences of extant rhinoceroses (Perissodactyla, Mammalia). *Mammal Research*, 64:397–409. doi:
813 10.1007/s13364-019-00427-4.
- 814 Hullot, M., Y. Laurent, G. Merceron, and P.-O. Antoine. 2021. Paleocology of the Rhinocerotidae (Mammalia,
815 Perissodactyla) from Béon 1, Montréal-du-Gers (late early Miocene, SW France): Insights from dental
816 microwear texture analysis, mesowear, and enamel hypoplasia. *Palaeontologia Electronica*, 24:1–26.
817 doi: 10.26879/1163.
- 818 Hutchinson, G. E. 1959. Homage to Santa Rosalia or why are there so many kinds of animals? *The American*
819 *Naturalist*, 93:145–159.
- 820 Inigo, C., and E. Cerdeño. 1997. The *Hispanotherium matritense* (Rhinocerotidae) from Córcoles (Guadalajara,
821 Spain): Its contribution to the systematics of the Miocene Iranotheriina. *Geobios*, 30:243–266. doi:
822 10.1016/S0016-6995(97)80232-X.
- 823 Janis, C. 2008. An Evolutionary History of Browsing and Grazing Ungulates; p. 21–45. *In* I. J. Gordon and H. H.
824 T. Prins (eds.), *The Ecology of Browsing and Grazing*, . Ecological Studies Springer, Berlin,
825 Heidelberg doi: 10.1007/978-3-540-72422-3_2.
- 826 Janis, C. M. 1988. An estimation of tooth volume and hypsodonty indices in ungulate mammals, and the
827 correlation of these factors with dietary preferences. *Memoires Du Museum National d' Histoire*
828 *Naturelle, serie C*, 53:367–387.
- 829 Jardine, P. E., C. M. Janis, S. Sahney, and M. J. Benton. 2012. Grit not grass: Concordant patterns of early origin
830 of hypsodonty in Great Plains ungulates and Glires. *Palaeogeography, Palaeoclimatology,*
831 *Palaeoecology*, 365–366:1–10. doi: 10.1016/j.palaeo.2012.09.001.
- 832 Jones, D. B., and L. R. G. DeSantis. 2017. Dietary ecology of ungulates from the La Brea tar pits in southern
833 California: A multi-proxy approach. *Palaeogeography, Palaeoclimatology, Palaeoecology*, 466:110–
834 127. doi: 10.1016/j.palaeo.2016.11.019.
- 835 Kaiser, T. M. 2009. *Anchitherium aurelianense* (Equidae, Mammalia): a brachyodont “dirty browser” in the
836 community of herbivorous large mammals from Sandelzhausen (Miocene, Germany). *Paläontologische*
837 *Zeitschrift*, 83:131.
- 838 Landman, M., D. S. Schoeman, and G. I. H. Kerley. 2013. Shift in Black Rhinoceros Diet in the Presence of
839 Elephant: Evidence for Competition? *PLOS ONE*, 8:e69771. doi: 10.1371/journal.pone.0069771.
- 840 Larramendi, A. 2015. Shoulder height, body mass, and shape of proboscideans. *Acta Palaeontologica Polonica*,
841 61:537–574.
- 842 Legendre, S., S. Montuire, O. Maridet, and G. Escarguel. 2005. Rodents and climate: A new model for
843 estimating past temperatures. *Earth and Planetary Science Letters*, 235:408–420. doi:
844 10.1016/j.epsl.2005.04.018.
- 845 Lopenen, L. 2020. Diets of Miocene proboscideans from Eurasia, and their connection to environments and
846 vegetation. Master Thesis, University of Helsinki, Finland, 54 p.
- 847 Louail, M., S. Ferchaud, A. Souron, A. E. C. Walker, and G. Merceron. 2021. Dental microwear textures differ
848 in pigs with overall similar diets but fed with different seeds. *Palaeogeography, Palaeoclimatology,*
849 *Palaeoecology*, 572:110415. doi: 10.1016/j.palaeo.2021.110415.
- 850 MacFadden, B. 1992. *Fossil Horses: Systematics, Paleobiology, and Evolution of the Family Equidae*,
851 Cambridge University Press. New York, p.
- 852 Maridet, O., and S. Sen. 2012. Les Cricetidae (Rodentia) de Sansan; p. 29–65. *In* *Mammifères de Sansan*. Vol.

- 853 203. Mémoires du Muséum Paris.
- 854 Maridet, O., G. Escarguel, L. Costeur, P. Mein, M. Huguéney, and S. Legendre. 2007. Small mammal (rodents
855 and lagomorphs) European biogeography from the Late Oligocene to the mid Pliocene. *Global Ecology*
856 *and Biogeography*, 16:529–544. doi: <https://doi.org/10.1111/j.1466-8238.2006.00306.x>.
- 857 Martin, C., I. Bentaleb, and P.-O. Antoine. 2011. Pakistan mammal tooth stable isotopes show paleoclimatic and
858 paleoenvironmental changes since the early Oligocene. *Palaeogeography Palaeoclimatology*
859 *Palaeoecology*, 311:19–29. doi: [10.1016/j.palaeo.2011.07.010](https://doi.org/10.1016/j.palaeo.2011.07.010).
- 860 Mead, A. J. 1999. Enamel hypoplasia in Miocene rhinoceroses (*Teleoceras*) from Nebraska: evidence of severe
861 physiological stress. *Journal of Vertebrate Paleontology*, 19:391–397.
- 862 Merceron, G., A. Kallend, A. Francisco, M. Louail, F. Martin, C.-A. Plastiras, G. Thiery, and J.-R. Boisserie.
863 2021. Further away with dental microwear analysis: Food resource partitioning among Plio-Pleistocene
864 monkeys from the Shungura Formation, Ethiopia. *Palaeogeography, Palaeoclimatology, Palaeoecology*,
865 572:110414. doi: [10.1016/j.palaeo.2021.110414](https://doi.org/10.1016/j.palaeo.2021.110414).
- 866 Merceron, G., A. Ramdarshan, C. Blondel, J.-R. Boisserie, N. Brunetiere, A. Francisco, D. Gautier, X. Milhet,
867 A. Novello, and D. Pret. 2016. Untangling the environmental from the dietary: dust does not matter.
868 *Proc. R. Soc. B*, 283 doi: [10.1098/rspb.2016.1032](https://doi.org/10.1098/rspb.2016.1032).
- 869 Muhlbachler, M. C., F. Rivals, N. Solounias, and G. M. Semprebon. 2011. Dietary change and evolution of
870 horses in North America. *Science*, 331:1178–1181. doi: [10.1126/science.1196166](https://doi.org/10.1126/science.1196166).
- 871 Niven, L. B., C. P. Egeland, and L. C. Todd. 2004. An inter-site comparison of enamel hypoplasia in bison:
872 implications for paleoecology and modeling Late Plains Archaic subsistence. *Journal of Archaeological*
873 *Science*, 31:1783–1794. doi: [10.1016/j.jas.2004.06.001](https://doi.org/10.1016/j.jas.2004.06.001).
- 874 Owen-Smith, N. R. 1988. *Megaherbivores: The Influence of Very Large Body Size on Ecology*. Cambridge
875 University Press, 392 p.
- 876 Prothero, D. R. 2005. *The Evolution of North American Rhinoceroses*. Cambridge University Press, 232 p.
- 877 Prothero, D. R., C. Guérin, and E. Manning. 1989. The history of the Rhinoceroidea; p. 322–340. *In* D. R.
878 Prothero and R. M. Schoch (eds.), *The Evolution of Perissodactyls*. Oxford University Press, New
879 York.
- 880 Rivals, F., G. Semprebon, and A. Lister. 2012. An examination of dietary diversity patterns in Pleistocene
881 proboscideans (*Mammuthus*, *Palaeoloxodon*, and *Mammot*) from Europe and North America as
882 revealed by dental microwear. *Quaternary International*, 255:188–195. doi:
883 [10.1016/j.quaint.2011.05.036](https://doi.org/10.1016/j.quaint.2011.05.036).
- 884 Rivals, F., N. E. Prilepskaya, R. I. Belyaev, and E. M. Pervushov. 2020. Dramatic change in the diet of a late
885 Pleistocene *Elasmotherium* population during its last days of life: Implications for its catastrophic
886 mortality in the Saratov region of Russia. *Palaeogeography, Palaeoclimatology, Palaeoecology*,
887 556:109898. doi: [10.1016/j.palaeo.2020.109898](https://doi.org/10.1016/j.palaeo.2020.109898).
- 888 Roohi, G., S. M. Raza, A. M. Khan, R. M. Ahmad, and M. Akhtar. 2015. Enamel Hypoplasia in Siwalik
889 Rhinocerotids and its Correlation with Neogene Climate. *Pakistan Journal of Zoology*, 47.
- 890 Rothschild, B. M., L. D. Martin, G. Lev, H. Bercovier, G. K. Bar-Gal, C. Greenblatt, H. Donoghue, M.
891 Spigelman, and D. Brittain. 2001. *Mycobacterium tuberculosis* Complex DNA from an Extinct Bison
892 Dated 17,000 Years before the Present. *Clinical Infectious Diseases*, 33:305–311. doi: [10.1086/321886](https://doi.org/10.1086/321886).
- 893 Sabol, M., and M. Kováč. 2006. Badenian palaeoenvironment, faunal succession and biostratigraphy: a case
894 study from northern Vienna Basin, Devínska Nová Ves-Bonanza site (Western Carpathians, Slovakia).
895 *Beiträge Zur Paläontologie*, 30:415–425.
- 896 Scott, R. S., P. S. Ungar, T. S. Bergstrom, C. A. Brown, F. E. Grine, M. F. Teaford, and A. Walker. 2005. Dental

- 897 microwear texture analysis shows within-species diet variability in fossil hominins. *Nature*, 436:693–
898 695. doi: 10.1038/nature03822.
- 899 Scott, R. S., P. S. Ungar, T. S. Bergstrom, C. A. Brown, B. E. Childs, M. F. Teaford, and A. Walker. 2006.
900 Dental microwear texture analysis: technical considerations. *Journal of Human Evolution*, 51:339–349.
901 doi: 10.1016/j.jhevol.2006.04.006.
- 902 Semprebon, G. M., and F. Rivals. 2007. Was grass more prevalent in the pronghorn past? An assessment of the
903 dietary adaptations of Miocene to Recent Antilocapridae (Mammalia: Artiodactyla). *Palaeogeography,*
904 *Palaeoclimatology, Palaeoecology*, 253:332–347. doi: 10.1016/j.palaeo.2007.06.006.
- 905 Semprebon, G. M., P. J. Sise, and M. C. Coombs. 2011. Potential bark and fruit browsing as revealed by
906 stereomicroscopic analysis of the peculiar clawed herbivores known as chalicotheres (Perissodactyla,
907 Chalicotherioidea). *Journal of Mammalian Evolution*, 18:33–55. doi: 10.1007/s10914-010-9149-3.
- 908 Semprebon, G. M., F. Rivals, and C. M. Janis. 2019. The Role of Grass vs. Exogenous Abrasives in the
909 Paleodietary Patterns of North American Ungulates. *Frontiers in Ecology and Evolution*, 7 doi:
910 10.3389/fevo.2019.00065.
- 911 Skinner, M. F., and J. D. Pruetz. 2012. Reconstruction of periodicity of repetitive linear enamel hypoplasia from
912 perikymata counts on imbricational enamel among dry-adapted chimpanzees (*Pan troglodytes verus*)
913 from Fongoli, Senegal. *American Journal of Physical Anthropology*, 149:468–482. doi:
914 10.1002/ajpa.22145.
- 915 Suckling, G., D. C. Elliott, and D. C. Thurley. 1986. The macroscopic appearance and associated histological
916 changes in the enamel organ of hypoplastic lesions of sheep incisor teeth resulting from induced
917 parasitism. *Archives of Oral Biology*, 31:427–439. doi: 10.1016/0003-9969(86)90016-6.
- 918 Tafforeau, P., I. Bentaleb, J.-J. Jaeger, and C. Martin. 2007. Nature of laminations and mineralization in
919 rhinoceros enamel using histology and X-ray synchrotron microtomography: potential implications for
920 palaeoenvironmental isotopic studies. *Palaeogeography, Palaeoclimatology, Palaeoecology*, 246:206–
921 227.
- 922 Tissier, J., P.-O. Antoine, and D. Becker. 2020. New material of *Epiaceratherium* and a new species of
923 *Mesaceratherium* clear up the phylogeny of early Rhinocerotidae (Perissodactyla). *Royal Society Open*
924 *Science*, 7:200633. doi: 10.1098/rsos.200633.
- 925 Tütken, T., T. M. Kaiser, T. Vennemann, and G. Merceron. 2013. Opportunistic Feeding Strategy for the Earliest
926 Old World Hysodont Equids: Evidence from Stable Isotope and Dental Wear Proxies. *PLOS ONE*,
927 8:e74463. doi: 10.1371/journal.pone.0074463.
- 928 Upex, B., and K. Dobney. 2012. Dental enamel hypoplasia as indicators of seasonal environmental and
929 physiological impacts in modern sheep populations: a model for interpreting the zooarchaeological
930 record. *Journal of Zoology*, 287:259–268. doi: 10.1111/j.1469-7998.2012.00912.x.
- 931 Van der Made, J. 2003. Suoidea (Artiodactyla); p. 308–327. *In* *Geology and paleontology of the Miocene Sinap*
932 *Formation, New York (Columbia University Press).*
- 933 Venables, W. N., and B. D. Ripley. 2002. *Modern Applied Statistics with S*, Springer. New York, p.
- 934 Wasserstein, R. L., and N. A. Lazar. 2016. The ASA Statement on p-Values: Context, Process, and Purpose. *The*
935 *American Statistician*, 70:129–133. doi: 10.1080/00031305.2016.1154108.
- 936 Wasserstein, R. L., A. L. Schirm, and N. A. Lazar. 2019. Moving to a World Beyond “ $p < 0.05$.” *The American*
937 *Statistician*, 73:1–19. doi: 10.1080/00031305.2019.1583913.
- 938 Westerhold, T., N. Marwan, A. J. Drury, D. Liebrand, C. Agnini, E. Anagnostou, J. S. K. Barnet, S. M. Bohaty,
939 D. D. Vleeschouwer, F. Florindo, T. Frederichs, D. A. Hodell, A. E. Holbourn, D. Kroon, V. Laurentino,
940 K. Littler, L. J. Lourens, M. Lyle, H. Pälike, U. Röhl, J. Tian, R. H. Wilkens, P. A. Wilson, and J. C.
941 Zachos. 2020. An astronomically dated record of Earth’s climate and its predictability over the last 66

- 942 million years. *Science*, 369:1383–1387. doi: 10.1126/science.aba6853.
- 943 Wickham, H. 2007. Reshaping data with the reshape package. *Journal of Statistical Software*, 21:1–20.
- 944 Wickham, H. 2011. ggplot2. *Wiley Interdisciplinary Reviews: Computational Statistics*, 3:180–185.
- 945 Wickham, H., R. François, L. Henry, and K. Müller. 2019. dplyr: A Grammar of Data Manipulation. *R Package*
946 Version 0.8.3, 13:2020.
- 947 Winkler, D. E., E. Schulz-Kornas, T. M. Kaiser, D. Codron, J. Leichliter, J. Hummel, L. F. Martin, M. Clauss,
948 and T. Tütken. 2020. The turnover of dental microwear texture: Testing the “last supper” effect in small
949 mammals in a controlled feeding experiment. *Palaeogeography, Palaeoclimatology, Palaeoecology*,
950 557:109930. doi: 10.1016/j.palaeo.2020.109930.
- 951 Xafis, A., J. Saarinen, K. Bastl, D. Nagel, and F. Grímsson. 2020. Palaeodietary traits of large mammals from
952 the middle Miocene of Gračanica (Bugojno Basin, Bosnia-Herzegovina). *Palaeobiodiversity and*
953 *Palaeoenvironments*, 100:457–477. doi: 10.1007/s12549-020-00435-2.
- 954 Zachos, J., M. Pagani, L. Sloan, E. Thomas, and K. Billups. 2001. Trends, rhythms, and aberrations in global
955 climate 65 Ma to present. *Science*, 292:686–693.
- 956